Journal Pre-proof

Neutrophil extracellular traps promote ΔNp63+ basal cell hyperplasia in chronic rhinosinusitis

Suha Lim, BSc, Roza Khalmuratova, MD, PhD, Yun Young Lee, BSc, Yi Sook Kim, BSc, Mingyu Lee, PhD, Na Kyeong Lee, BSc, Se-Na Kim, PhD, Young Bin Choy, PhD, Chun Gwon Park, PhD, Dae Woo Kim, MD, PhD, Hyun-Woo Shin, MD, PhD

PII: S0091-6749(23)01478-1

DOI: https://doi.org/10.1016/j.jaci.2023.11.016

Reference: YMAI 16173

To appear in: *Journal of Allergy and Clinical Immunology*

Received Date: 14 February 2023

Revised Date: 6 November 2023

Accepted Date: 10 November 2023

Please cite this article as: Lim S, Khalmuratova R, Lee YY, Kim YS, Lee M, Lee NK, Kim S-N, Choy YB, Park CG, Kim DW, Shin H-W, Neutrophil extracellular traps promote ΔNp63+ basal cell hyperplasia in chronic rhinosinusitis, *Journal of Allergy and Clinical Immunology* (2023), doi: https://doi.org/10.1016/j.jaci.2023.11.016.

This is a PDF file of an article that has undergone enhancements after acceptance, such as the addition of a cover page and metadata, and formatting for readability, but it is not yet the definitive version of record. This version will undergo additional copyediting, typesetting and review before it is published in its final form, but we are providing this version to give early visibility of the article. Please note that, during the production process, errors may be discovered which could affect the content, and all legal disclaimers that apply to the journal pertain.

© 2023 Published by Elsevier Inc. on behalf of the American Academy of Allergy, Asthma & Immunology.

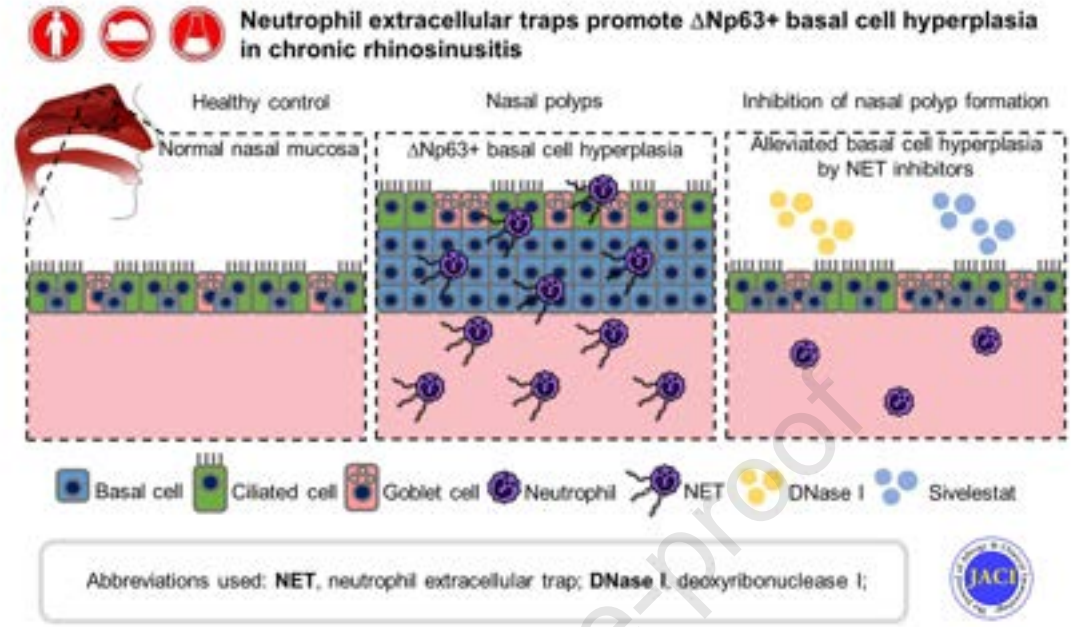

Journal Pre-proof

Journal Pre-proof

Neutrophil extracellular traps promote ΔNp63+ basal cell hyperplasia in chronic rhinosinusitis

Authors: Suha Lim, BSc,[1,2,3] Roza Khalmuratova, MD, PhD,[1] Yun Young Lee, BSc,[6] Yi Sook Kim, BSc,[1,2,3] Mingyu Lee, PhD,[1,2,3,11] Na Kyeong Lee, BSc,[7,8] Se-Na Kim, PhD,[9] Young Bin Choy, PhD,[6] Chun Gwon Park, PhD,[7,8] Dae Woo Kim, MD, PhD[5,10] and Hyun-Woo Shin, MD, PhD[1,2,3,4,5]*

Affiliations:

[1]Obstructive Upper airway Research (OUaR) Laboratory, Department of Pharmacology, Seoul National University College of Medicine, Seoul, Korea

[2]Department of Biomedical Sciences, Seoul National University Graduate School, Seoul, Korea

[3]Cancer Research Institute, Seoul National University College of Medicine, Seoul, Korea

[4]Department of Otorhinolaryngology-Head and Neck Surgery, Seoul National University Hospital, Seoul, Korea

[5]Sensory Organ Research Institute, Seoul National University Medical Research Center, Seoul, Korea

[6]Department of Biomedical Engineering, Seoul National University College of Medicine, Seoul, Korea

[7]Department of Biomedical Engineering, SKKU Institute for Convergence, Sungkyunkwan University (SKKU), Suwon, Korea

[8]Department of Intelligent Precision Healthcare Convergence, SKKU Institute for Convergence, Sungkyunkwan University (SKKU), Suwon, Korea

[9]Research and Development Center, MediArk Inc., Cheongju, Korea

[10]Department of Otorhinolaryngology-Head and Neck Surgery, Seoul National University College of Medicine, Seoul National University Boramae Medical Center, Seoul, Korea

Journal Pre-proof

[11]Present address: Division of Allergy and Clinical immunology, Brigham and Women's Hospital and Department of Medicine, Harvard Medical School, Boston, USA

[*]To whom correspondence should be addressed.

Correspondence to:

Hyun-Woo Shin, M.D., Ph.D.

Department of Pharmacology, Seoul National University College of Medicine, 103 Daehak-ro, Jongno-gu, Seoul 03080, Korea. Phone: +82-2-740-8285, Fax: +82-2-745-7996, E-mail: charlie@snu.ac.kr

Declaration of interests

The authors have declared that no conflict of interest exists.

Journal Pre-proof

ABSTRACT

Background: Neutrophil extracellular traps (NETs) are observed in chronic rhinosinusitis (CRS), although their role remains unclear.

Objective: This study aimed to investigate the influence of NETs on the CRS epithelium.

Methods: Forty-five sinonasal biopsy specimens were immunofluorescence-stained to identify NETs and p63+ basal stem cells. We treated human nasal epithelial cells with NETs and studied them with immunofluorescence staining, western blotting, and quantitative real-time polymerase chain reaction. NET inhibitors were administered to a murine neutrophilic nasal polyp (NP) model.

Results: NETs existed in tissues in patients with CRS with NPs, especially in non-eosinophilic NP tissues. p63+ basal cell expression had a positive correlation with the release of NETs. NETs induced the expansion of Ki-67+p63+ cells. We found that ΔNp63, an isoform of p63, was mainly expressed in the nasal epithelium and controlled by NETs. Treatment with deoxyribonuclease (DNase) I or Sivelestat (NET inhibitors) prevented the overexpression of ΔNp63+ epithelial stem cells and reduced polyp formation.

Conclusions: These results reveal that NETs are implicated in CRS pathogenesis via basal cell hyperplasia. Our study suggests a novel possibility of treating CRS by targeting NETs.

Key Messages:

- NETs close to the epithelial cells are observed in patients with CRSwNP.
- NETs induce ΔNp63+ basal cell expansion and epithelial thickness.
- DNase I and Sivelestat effectively reduce the number of nasal polyps through eliminating NETs.

Journal Pre-proof

Capsule Summary: NETs cause basal cell hyperplasia in nearby nasal epithelial cells. Targeting NETs can be a novel therapeutic strategy for severe CRS.

Keywords: Chronic rhinosinusitis, neutrophil extracellular traps, hyperplasia, ΔNp63, nasal polyps

Abbreviations:

ARDS: Acute respiratory distress syndrome

ALI: Air-liquid interface

CitH3: Citrullinated histone H3

CRS: Chronic rhinosinusitis

CRSsNP: Chronic rhinosinusitis without nasal polyps

CRSwNP: Chronic rhinosinusitis with nasal polyps

ΔN: N-terminal truncated domain

DEX: Dexamethasone

DNase: Deoxyribonuclease

EDN: Eosinophil-derived neurotoxin

EET: Eosinophil extracellular traps

EMT: Epithelial-to-mesenchymal transition

hNECs: Human nasal epithelial cells

LPS: Lipopolysaccharide

MPO: Myeloperoxidase

Journal Pre-proof

NE: Neutrophil elastase

NET: Neutrophil extracellular traps

PMA: Phorbol 12-myristate 13-acetate

ROS: Reactive oxygen species

TA: N-terminal transactivation domain

TGF-β: Transforming growth factor-β

UP: Uncinate process

YAP: Yes-associated protein

Journal Pre-proof

INTRODUCTION

Chronic rhinosinusitis (CRS) is a heterogeneous chronic inflammation of the paranasal sinuses and nasal mucosa, affecting around 10% of the population worldwide. CRS can be classified according to the presence of nasal polyps (NP) as CRS without nasal polyps (CRSsNP) and CRS with nasal polyps (CRSwNP). CRSwNP has high recurrence rates and comorbid asthma.[1] The endotypes of CRS are subdivided into eosinophilic and non-eosinophilic CRS.[2] Previously, eosinophilic CRSwNP with type 2 inflammation was well known as a severe type of CRS.[3, 4] However, recent studies have reported that mixed granulocytic endotype, characterized by an increase in both eosinophils and neutrophils, is more prevalent of refractoriness and recurrence.[5-7] In addition, neutrophil extracellular traps (NETs) have been discovered and can exacerbate asthma, COPD and CRS.[8-10] Corticosteroids are typical anti-inflammatory drugs especially suppressing type 2 inflammation and eosinophils, but neutrophils may contribute to resistant to the steroids.[11, 12] Several biologics approved for CRS also targeted type 2 inflammation including interleukin (IL)-4, IL-5, IL-13, and immunoglobulin E.[13, 14] Nonetheless, treatments for neutrophilic inflammation in CRS are limited. Therefore, understanding and targeting neutrophils in upper airway could be an important therapeutic strategy.

Neutrophils form the first line of innate immune defense against pathogens.[15] Neutrophils extrude cytosolic and nuclear proteins and DNA via a conserved cell death process referred to as NETosis. This cell death relies on generating reactive oxygen species (ROS) via the nicotinamide adenine dinucleotide phosphate oxidase.[16] ROS activates peptidyl arginine deiminase 4, an enzyme that citrullinates histones resulting in the decondensation of DNA.[17] In addition, neutrophil elastase (NE) and myeloperoxidase (MPO) translocate from the neutrophil granules into the nucleus by the ROS. NE and MPO in nucleus also dissociate histones and DNA.[18] Thus, extracellular DNA with citrullinated histones and neutrophil granule proteins are used as the marker of NETosis.[19, 20] NETs play a role in immobilizing and killing pathogens, but over-releasing NETs exacerbates various diseases by causing cell damage, inflammation, cell proliferation, or the recruitment of other immune cells.[21] As mentioned above, increasingly many reports have reported observing NETs in CRS.[9, 22] Cao et al.[22] found upregulated LL-37 mRNA and

protein levels in NP tissues and showed that LL-37 induced NET formation. Neutrophilic granules and NETs contain LL-37, potentially facilitating a positive feedback loop in NET release. Several studies have investigated the pro-inflammatory roles of NETs. Cytokine screening was performed in nasal tissue homogenates, and high levels of IL-8, IL-6, tumor necrosis factor-α, and granulocyte colony-stimulating factor were identified in the NET-high cluster.[23] NETs can have diverse influences on the upper airway, but the effect of NETs on the CRS epithelium has not been studied.

Here, we explored the influence of NETs on airway epithelial cells in CRS, and found that NETs existed in abundance near epithelial cells using nasal tissues from CRS patients. It was also shown that NETs can induce basal cell proliferation. This finding was also observed and evaluated in a mouse neutrophilic NP model using NET inhibitors.

METHODS

Human subjects

Sinonasal and polyp tissues for staining were collected after obtaining written informed consent with approval from the Institutional Review Board of Seoul Metropolitan Government Seoul National University Boramae Medical Center (No. 06-2012-109). The demographic characteristics of the patients are summarized in Table E1. Sinonasal or polyp tissues were obtained from patients with CRS from functional endoscopic sinus surgery (FESS). The diagnosis of sinusitis or nasal polyposis was determined in subjects with CRS by personal medical history, physical examination, nasal endoscopy, and computed tomography findings of the sinuses following the European position paper on rhinitis and nasal polyps 2020 guidelines.[3] The exclusion criteria were as follows: 1) age younger than 18 years; 2) previous within 4 weeks treatment with antibiotics, systemic or topical corticosteroids; 3) unilateral rhinosinusitis, antrochoanal polyp, allergic fungal sinusitis, cystic fibrosis, or immotile ciliary disease. We acquired uncinate process (UP) from control subjects, patients with CRSsNP and CRSwNP. Control samples were collected from patients without any sinonasal diseases, mucopurulent secretions, or swelling during other rhinologic procedures such as lacrimal duct, orbital decompression, or skull base

surgery.

Samples were fixed in 4% formaldhyde and embedded in paraffin for histologic analysis, and sectioned with 4μm thickness. We classified it as eosinophilic NP when the percent of eosinophils among all immune cells in tissues exceed 10 %.

Isolation and air-liquid interface culture of primary human nasal epithelial cells

Nasal tissues were sampled after obtaining informed consent with approval from the Institutional Review Board of Seoul National University Boramae Medical Center (No. 10-2020-21). Nasal mucosa from healthy control subjects was treated with 0.1% protease (type XIV) (Sigma, Saint Louis, MO, USA) for 1 hour, after which human nasal epithelial cells (hNECs) were scraped. Cells were washed with Dulbecco modified Eagle medium (DMEM) and cultured with bronchial epithelial cell growth basal medium (BEGM) (Lonza, Basel, Switzerland) with all supplements. Additional materials were described in a previous study.[24] Cells were seeded on a 6.5 mm^2 transwell with 0.4-μm-pore polyester membrane inserts (Corning Inc., Corning, NY, USA) at a density of 5×10^4 cells per well. Cells were grown for 2 days in a 1:1 mixture of BEGM and DMEM under submerged conditions. After 2 days, the apical medium was removed to make an air-liquid interface (ALI). The ALI culture system was maintained for 14 days to differentiate epithelial cells. The medium and NETs were changed every other day. For the NET inhibitor study, NETs were pre-incubated with deoxyribonuclease (DNase) I (10 U/mL) (Invitrogen, Waltham, MA, USA) or Sivelestat (10 μM) (Tocris, Bristol, UK) for 1 hour at 37℃.

Neutrophil isolation and NET formation

Human peripheral blood was obtained from healthy donors who were enrolled in an Institutional Review Board approved study at Seoul National University Hospital (1904-041-1024). Blood was collected in EDTA coating tubes and then was isolated for neutrophils using the Easysep direct human

neutrophil isolation kit (Stem Cell, Vancouver, Canada). After isolation, neutrophils were suspended in a Roswell Park Memorial Institute Medium 1640 (Welgene, Gyeongsan, Korea) with 1% fetal bovine serum.

For NET formation, human blood neutrophils were seeded on 55 cm^2 polystyrene culture dishes at a density of 5×10^6 cells per well and stimulated with 100 nM phorbol 12-myristate 13-acetate (PMA) (Tocris, Bristol, UK) for 3 hours at 37℃. After NET formation, the medium was removed and washed carefully with PBS without Ca^{2+} and Mg^{2+} to remove PMA. Then, NETs were treated with the AluI restriction enzyme (10 U/mL) (New England Biolabs, Ipswich, MA, USA) in BEGM medium for 30 minutes at 37℃. The NET-containing medium was collected and centrifuged to eliminate cell debris. For NET quantification, the DNA concentration was measured using a Quant-iT Picogreen dsDNA assay kit (Thermo Fisher, Eugene, OR, USA). The hNECs were incubated with NETs at a concentration of 100 ng/mL.

Statistical analysis

At least 5 independent experiments were performed. Data points were represented as means ± SEM. Differences between groups were assessed by the Wilcoxon signed rank test or the Mann-Whitney U test. Correlations between the 2 groups were analyzed by the Spearman's rank correlation. P values are indicated as: n.s., not significant; *P<0.05; **P<0.01; ***P<0.001. Statistics were conducted using SPSS ver. 26.0 (SPSS Inc., Chicago, IL, USA).

Additional methods are reported in the Online Repository.

RESULTS

NETotic cells are abundant in patients with CRSwNP

Journal Pre-proof

To investigate the existence of NETs by subtypes of CRS, we used human nasal tissues from patients with CRSsNP (UP tissues, n = 11), patients with CRSwNP (UP tissues, n = 9), eosinophilic NP (NP tissues, n = 8), non-eosinophilic NP (NP tissues, n = 10), and healthy control subjects (UP tissues, n = 7) for immunofluorescence staining. NE and citrullinated histone H3 (CitH3) were co-stained, and double-positive cells were counted to quantify NETs (Fig 1, *A* and *B*).[20, 25] NETs existed in patients with CRSwNP, and were especially highly present in non-eosinophilic NP tissues. We expected NE- CitH3+ cells to be eosinophil extracellular traps (EETs), so we verified EETs in nasal tissues (Fig E1). Next, we examined the proteins from nasal secretions using LC-MS/MS analysis to estimate extracellular proteins. Nasal secretions were obtained from controls (n = 23), patients with CRSsNP (n = 24), and patients with CRSwNP (n = 22). The CRSwNP group showed higher expressions of NE, MPO (neutrophil granule proteins), histone H2B, and histone H3 (nuclear proteins) (Fig 1, *C*). The neutrophil granule proteins were positively correlated with histone proteins (Fig 1, *D*). We divided the patients into two groups based on the median value of eosinophil-derived neurotoxin (EDN): EDN high is considered as eosinophilic, and EDN low as non-eosinophilic (Fig E2). As shown in immunofluorescence results (Fig 1, *B*), the levels of NE, MPO, and histone H3 were elevated in CRSwNP (EDN low) group compared to control. In addition, CRSwNP (EDN low) group showed a higher tendency of NE, MPO and histone H3 than CRSwNP (EDN high), but a statistical difference was not found. Taken together, patients with CRSwNP had NET-releasing neutrophils.

NETs are located adjacent to the nasal epithelium

While exploring NETs in nasal tissues, we found that neutrophils and NETs were located nearby epithelial cells. We measured the distance between NETs and the basement membrane to clarify the proximity of NETs to the epithelium (Fig 2, *A*). Most NETs were within 50 μm of epithelial cells (Fig 2, *B*). Furthermore, neutrophils accumulated in the epithelial region and release NETs (Fig 2, *A* and *B*). Thus, we expected that neighboring NETs could affect epithelial cells.

Journal Pre-proof

Journal Pre-proof

NET-rich nasal tissues show basal cell hyperplasia

We observed that NET-high tissues seemed to show epithelial thickening. In addition, several studies have revealed that NETs contributed to cell proliferation. In one study, neutrophil proteases contained in NETs (NE and matrix metalloproteinase 9) initiated dormant cancer cell proliferation through laminin cleavage, which activated integrin signaling.[26] Another study indicated that NETs promoted gastric cancer cell proliferation dependent on transforming growth factor-β (TGF-β) signaling.[27] According to a single-cell transcriptome analysis, epithelial cell types in NPs showed an increase in basal cells and a decrease in ciliated and glandular cells compared with non-polyp tissues.[28] Thus, we hypothesized NETs affect basal cell proliferation, leading to basal cell hyperplasia. We stained NETs with p63 as a basal cell marker in CRS patients' tissues (Fig 3, *A*). The basal cell layer was correlated with the number of NETs (Fig 3, *B*). Because most of NETs existed in non-eosinophilic NP, we examined the correlation analysis in non-eosinophilic NP tissues (Fig E3, *A* and *B*). Likewise, the number of basal cells had a positive correlation with NETs (Fig 3, *C*). Therefore, NETs may impact basal cell hyperplasia in nasal tissues.

NETs stimulate basal cell proliferation in primary hNECs

To determine whether NETs induce basal cell expansion in differentiated hNECs, we utilized an ALI culture system. After differentiation, we treated NETs in the lower chamber of a transwell for 4 days (Fig 4, *A*). Then, we performed p63 staining for basal cells and E-cadherin staining to identify the cell structure. We focused on the lateral side of cells to measure the cell thickness (Fig 4, *B*). NETs were associated with a significantly higher number of basal cells and epithelial cell thickness (Fig 4, *C* and *D*). In addition, basal cell number and epithelial cell thickness increased in a time-dependent manner from day 0 to day 8 after the treatment of NETs (Fig E4). Moreover, using Z-stack images, we reconfirmed the thickness of NET-treated hNECs (Fig E5, *A* and *B*). Ki-67, expressing in cycling cells (G1, S, G2, and M phases) but not in resting cells (G0 phase),[29] was stained to assess basal cell proliferation (Fig 4, *E*). The proportion of Ki-67+ p63+ cells was higher in the areas with NETs (Fig 4,

Journal Pre-proof

F). We also showed Ki-67+ cells at low magnification and counted total cell number (Fig E5, *C* and *D*). There are six major p63 isoforms of p63 due to different promoters, one with the N-terminal transactivation domain (TAp63) and the other lacking the N-terminal transactivation domain (ΔNp63), each of which has α, β, and γ isoforms as alternative splicing of the C-terminal.[30] ΔNp63 is detected in various epithelial tissues such as skin, breast and prostate.[31] Olfactory epithelium[32] and nasal epithelium[33] also contain ΔNp63, but TAp63 is expressed in some bronchiolar epithelial cells[34] and skin-derived precursors.[35] To elucidate which isoform of p63 is present in hNECs, TAp63 and ΔNp63 mRNA levels were measured (Fig 4, *G*). We established that ΔNp63 is the major isoform of hNECs. Next, we carried out western blotting to determine which C-terminal domain of ΔNp63 is regulated by NETs (Fig 4, *H*). As a result, all isoforms of ΔNp63 (α, β, and γ) were upregulated by NETs (Fig 4, *I*). These data suggest that NETs promote ΔNp63+ basal cell proliferation, resulting in epithelial thickening.

NET inhibitors prevent polyp formation in a murine neutrophilic polyp model

To confirm whether NET-induced basal cell proliferation has an effect on the pathogenesis of CRSwNP, we investigated a mouse neutrophilic polyp model. In our previous study, we established mouse neutrophilic NP models.[36] In this study, we used a lipopolysaccharide (LPS)-mediated neutrophilic NP model because it revealed the highest degree of neutrophil infiltration. To evaluate the role of NET inhibition, we used DNase I (coated on nanoparticles) and Sivelestat (a NE inhibitor). DNase I degrades NETs structurally. Sivelestat blocks NE, which is crucial for NET formation.[37] Dexamethasone (DEX) is a type of corticosteroid that is used to reduce inflammation. We added DEX treated group for positive control as a conventional treatment.[38-41] Sivelestat and DEX blocked polyp formation efficiently (Fig 5, *A*). The DNase I treated group was not significantly different in polyp formation, but the mean number of polyps decreased by around half (Fig 5, *B* and *C*). Next, we quantified the number of neutrophils and NETs. Sivelestat inhibited neutrophil infiltration and NET formation most effectively. DNase I also reduced neutrophil infiltration and NET formation as much as

DEX (Fig 5, *D, E* and *F*). Altogether, NET inhibitors reduced nasal polypoid lesions and neutrophilic inflammation.

Inhibition of NETs suppresses basal cell expansion in the mice tissues

Based on our histologic results in humans, we sought to identify whether basal cell hyperplasia was also observed in the mouse NP model. The neutrophilic NP model showed a markedly higher level of p63 and ΔNp63+ epithelial cells (Fig 6, *A* and *C*). We also assessed the role of NET inhibitors in regulating p63 and ΔNp63 *in vivo*. Consistent with NETs, the overexpression of ΔNp63+ basal cells decreased in response to Sivelestat. DNase I and DEX also prevented p63+ basal cell hyperplasia, although the number of ΔNp63+ cells was not significantly different (Fig 6, *B* and *D*). NET inhibitors also decreased the expression of goblet cells and eosinophil infiltration (Fig E6, *A* and *B*). Last, we evaluated the impact of NET inhibitors on hNECs. DNase I or Sivelestat were pre-incubated with NETs for 1 hour before treating the NETs in hNECs for 4 days (Fig 6, *E*). DNase I and Sivelestat restored the number of p63+ cells and epithelial thickness, although Sivelestat did not lead to a significant decrease in epithelial thickness (Fig 6, *F* and *G*). Consequently, NETs influenced basal cell growth, and repression of NETs alleviated NP formation.

DISCUSSION

In this study, we found that NETs were located adjacent to the basement membrane and epithelial cell layer. We observed that NETs were correlated with basal cell hyperplasia and identified NETs as a key regulator of basal cell proliferation. The LPS-induced neutrophilic NP mouse model showed ectopic expression of basal cells, which was alleviated in response to treatment with NET inhibitors. Moreover, NET inhibitors markedly prevented polyp formation. Interestingly, the administration of Sivelestat was more effective than steroid treatment for reducing polyp formation (Fig 5, *B*). Taken together, inhibiting NETs can be a novel therapeutic for neutrophilic airway diseases.

Journal Pre-proof

Sivelestat inhibits the activity of NE, which translocates into the nucleus and stimulates the decondensation of chromatin by proteolytic activity. Sivelestat has been approved in Korea and Japan for the treatment of acute respiratory distress syndrome (ARDS).[42] Moreover, there are diverse NE inhibitors under clinical trials for chronic obstructive pulmonary disease, cystic fibrosis, ARDS, COVID-19, and bronchiectasis.[43] Based on our results, we expect Sivelestat to be clinically meaningful in upper airway diseases. DNase I (dornase alfa, Pulmozyme) was approved by the US Food and Drug Administration in 1993 for the treatment of cystic fibrosis.[44] DNase I has also been used to treat other respiratory conditions, including bronchiolitis, although it did not improve clinical outcomes.[45] Because DNase I degrades extracellular DNA after NET formation, it may fail to clear all of the NET components. We previously reported that PLGA nanoparticles remained present at 21 hours in sinonasal cavity and enhanced the activity of resveratrol.[46] Thus, we used DNase I-coated PLGA nanoparticles to prolong the maintenance of DNase I in the nasal cavity. In our *in vivo* experiment, DEX exhibited a therapeutic effect somewhat. This is probably because our mouse model did not have simply neutrophilic inflammation but rather neutrophilic one combined with eosinophilic inflammation. We have previously used the OVA+SEB, which serves as an eosinophilic NP model.[39, 47, 48] To enhance neutrophil infiltration, we additionally treated LPS and evaluated them in our previous trial.[36] Nevertheless, this neutrophilic NP model still exhibited substantial eosinophil infiltration (Fig E6, *B*), indicating that DEX would have had some effect. One study reported that *S. aureus*-induced NETs suppressed by DEX,[49] but in most cases, DEX did not directly inhibit NET formation.[50, 51] Despite this, animal experiments showed that DEX reduced NETs in bronchoalveolar lavage fluid.[52, 53] Consistently, patients with daily inhaled corticosteroids had lower plasma NET levels than those without in chronic lung diseases.[54] Overall, steroids may indirectly inhibit NET formation.

Epithelial hyperplasia is one of the hallmarks of epithelial cells in CRS patients. Studies have found that epithelial hyperplasia is present in around 74% of patients with CRSwNP.[55, 56] Kaneko et al.[33] showed that p63 and ΔNp63 levels were elevated in nasal tissues from patients with CRS, and the inhibition of p63 and ΔNp63 recovered tight junctions and cilia in hNECs. ΔNp63 is expressed in

Journal Pre-proof

bronchial,[57] olfactory,[58] and nasal epithelium.[33] It was known that ΔNp63 could control: 1) proliferation; 2) fate specification; 3) morphogenesis and differentiation; 4) senescence; 5) cell-cell, cell-matrix interaction; and 6) survival and activities of epithelial stem cells or progenitor cells.[59, 60] A histological analysis defined the upregulation of p63 and ΔNp63 in CRS, and the inhibition of p63 and ΔNp63 reinforced epithelial barrier functions with ciliogenesis in hNECs.[33] In agreement with this, the overexpression of p63+ basal cells was found to be accompanied by reduced quantities of ciliated and secretory cells in single-cell RNA sequencing data analysis.[28] Hence, basal cell hyperplasia is deleterious to airway epithelial function. One particular point of curiosity is the variability in the expression of ΔNp63 c-terminals among patients (Fig 4, *H*). There are few studies on p63 C-terminal isoforms but the effect of ΔNp63α on cell senescence an aging has been reported.[61, 62] Therefore, we observed ΔNp63 in control patients in the order of age (Fig E7). Interestingly, 19 and 27 aged patients highly expressed ΔNp63α, whereas 64 and 71 aged patients predominantly expressed ΔNp63β and ΔNp63γ. It is consistent with previous studies that the loss of ΔNp63α induces proliferative cell senescence.

Beyond cell proliferation, NETs could play other roles in respiratory epithelium. Recent studies have reported that NETs can induce not only type 3 immune responses, but also type 2 immunity.[63, 64] DNA released by NETs exacerbated rhinovirus-induced type 2 immune responses in allergic asthma.[63] Radermecker et al.[64] found that CXCR4-high neutrophils released NETs in allergic asthma, and the inhibition of NETs decreased IL-5, IL-4, and IL-13. Thus, the suppression of NETs may be effective at reducing type 2 inflammation in the upper airway. NETs are also among the main inducers of epithelial-to-mesenchymal transition (EMT), which refers to the loss of tight junctions and epithelial polarity and the emergence of mesenchymal cell features.[65] NETs' role in the EMT has been studied in cancers[66, 67] and COVID-19.[68] Diverse investigations have established the importance of the EMT in CRS. IFN-γ increased EMT markers in hNECs via p38, ERK signaling pathway.[24] Air pollutants are also key factors in promoting the EMT. Cigarette smoke was found to induce the EMT through TGF-β activation.[69] Diesel exhaust particles also promoted EMT by inducting the zinc finger E-box binding homeobox 2

transcription factor.[70] These studies imply that NETs may also exacerbate CRS through the EMT. Therefore, further research on the effects of NETs in the upper airway will be needed.

This study has several limitations. First, various stimuli trigger NET formation, but the main inducer of NETs in the respiratory tract remains unclear. Second, the small number of participants is also a limitation. Third, the molecular mechanisms of NET-derived p63 amplification need future research. Although it was not confirmed in this study, several signaling pathways activated by NETs are linked with basal cell proliferation factors. Zhao et al.[71] discovered that Yes-associated protein (YAP) regulates pseudostratified epithelium through physical interactions with p63, the cardinal transcription factor of basal stem cells. Consistent with the study, nuclear YAP was observed in nasal tissues with basal cell hyperplasia.[72] Another candidate as a signaling pathway is Wnt/β-catenin. ΔNp63-mediated Wnt/β-catenin signaling activation leads to basal cell expansion, whereas the proportion of ciliated and club cells was decreased by inhibiting differentiation in respiratory epithelial cells.[73] NE cleaves the junctional protein VE-cadherin, causing the endothelial-to-mesenchymal transition via β-catenin signaling.[74] Accordingly, NET-activating β-catenin might promote ΔNp63+ cells.

In conclusion, our study suggests that NETs may induce basal cell proliferation via upregulating ΔNp63 positivity and may contribute to NP formation in CRS. Considering that the inhibition of NETs *in vivo* sufficiently decreased ΔNp63 overexpression and subsequent nasal polypogenesis, targeting NETs could be a novel therapeutic strategy in CRS and NP.

Author's contributions

Conceptualization: H.-W. S.; methodology: S.L., R.K., Y.Y.L., Y.S.K., M.L., N.K.L., S.-N.L., C.G.P.; investigation: S.L., R.K., Y.S.K., H.-W.S.; animal experiments: S.L., R.K.; formal analysis and interpretation of data: S.L., H.-W.S.; resources: D.-W.K., Y.B.C, C.G.P.; writing – original draft: S.L.; writing – review and editing: S.L., D.-W.K., H.-W.S.; supervision: H.-W.S.; funding acquisition: H.-W.S.

Journal Pre-proof

Acknowledgement

This work was supported by grants from the National Research Foundation of Korea (2022R1A2C2006075 and 2022R1A4A3034038 to H.-W.S.)

Journal Pre-proof

REFERENCES

1. Calus L, Van Bruaene N, Bosteels C, Dejonckheere S, Van Zele T, Holtappels G, et al. Twelve-year follow-up study after endoscopic sinus surgery in patients with chronic rhinosinusitis with nasal polyposis. Clin Transl Allergy. 2019;9:30.
2. Payne SC, Early SB, Huyett P, Han JK, Borish L, Steinke JW. Evidence for distinct histologic profile of nasal polyps with and without eosinophilia. Laryngoscope. 2011;121(10):2262-7.
3. Fokkens WJ, Lund VJ, Hopkins C, Hellings PW, Kern R, Reitsma S, et al. European Position Paper on Rhinosinusitis and Nasal Polyps 2020. Rhinology. 2020;58(Suppl S29):1-464.
4. Lou H, Zhang N, Bachert C, Zhang L. Highlights of eosinophilic chronic rhinosinusitis with nasal polyps in definition, prognosis, and advancement. Int Forum Allergy Rhinol. 2018;8(11):1218-25.
5. Succar EF, Li P, Ely KA, Chowdhury NI, Chandra RK, Turner JH. Neutrophils are underrecognized contributors to inflammatory burden and quality of life in chronic rhinosinusitis. Allergy. 2020;75(3):713-6.
6. Kim DK, Kim JY, Han YE, Kim JK, Lim HS, Eun KM, et al. Elastase-Positive Neutrophils Are Associated With Refractoriness of Chronic Rhinosinusitis With Nasal Polyps in an Asian Population. Allergy Asthma Immunol Res. 2020;12(1):42-55.
7. Delemarre T, Bochner BS, Simon HU, Bachert C. Rethinking neutrophils and eosinophils in chronic rhinosinusitis. J Allergy Clin Immunol. 2021;148(2):327-35.
8. Ray A, Kolls JK. Neutrophilic Inflammation in Asthma and Association with Disease Severity. Trends Immunol. 2017;38(12):942-54.
9. Delemarre T, Holtappels G, De Ruyck N, Zhang N, Nauwynck H, Bachert C, et al. A substantial neutrophilic inflammation as regular part of severe type 2 chronic rhinosinusitis with nasal polyps. J Allergy Clin Immunol. 2021;147(1):179-88 e2.
10. Grabcanovic-Musija F, Obermayer A, Stoiber W, Krautgartner WD, Steinbacher P, Winterberg N, et al. Neutrophil extracellular trap (NET) formation characterises stable and exacerbated COPD and correlates with airflow limitation. Respir Res. 2015;16(1):59.
11. Green RH, Brightling CE, Woltmann G, Parker D, Wardlaw AJ, Pavord ID. Analysis of induced sputum in adults with asthma: identification of subgroup with isolated sputum neutrophilia and poor response to inhaled corticosteroids. Thorax. 2002;57(10):875-9.
12. Wen W, Liu W, Zhang L, Bai J, Fan Y, Xia W, et al. Increased neutrophilia in nasal polyps reduces the response to oral corticosteroid therapy. J Allergy Clin Immunol. 2012;129(6):1522-8 e5.
13. Bachert C, Marple B, Schlosser RJ, Hopkins C, Schleimer RP, Lambrecht BN, et al. Adult chronic rhinosinusitis. Nat Rev Dis Primers. 2020;6(1):86.
14. Yao Y, Zeng M, Liu Z. Revisiting Asian chronic rhinosinusitis in the era of type 2 biologics. Clin Exp Allergy. 2022;52(2):231-43.
15. Brinkmann V, Reichard U, Goosmann C, Fauler B, Uhlemann Y, Weiss DS, et al. Neutrophil extracellular traps kill bacteria. Science. 2004;303(5663):1532-5.

Journal Pre-proof

16. Fuchs TA, Abed U, Goosmann C, Hurwitz R, Schulze I, Wahn V, et al. Novel cell death program leads to neutrophil extracellular traps. J Cell Biol. 2007;176(2):231-41.
17. Wang Y, Wysocka J, Sayegh J, Lee YH, Perlin JR, Leonelli L, et al. Human PAD4 regulates histone arginine methylation levels via demethylimination. Science. 2004;306(5694):279-83.
18. Papayannopoulos V, Metzler KD, Hakkim A, Zychlinsky A. Neutrophil elastase and myeloperoxidase regulate the formation of neutrophil extracellular traps. J Cell Biol. 2010;191(3):677-91.
19. Yang L, Liu Q, Zhang X, Liu X, Zhou B, Chen J, et al. DNA of neutrophil extracellular traps promotes cancer metastasis via CCDC25. Nature. 2020;583(7814):133-8.
20. Knackstedt SL, Georgiadou A, Apel F, Abu-Abed U, Moxon CA, Cunnington AJ, et al. Neutrophil extracellular traps drive inflammatory pathogenesis in malaria. Sci Immunol. 2019;4(40).
21. Cahilog Z, Zhao H, Wu L, Alam A, Eguchi S, Weng H, et al. The Role of Neutrophil NETosis in Organ Injury: Novel Inflammatory Cell Death Mechanisms. Inflammation. 2020;43(6):2021-32.
22. Cao Y, Chen F, Sun Y, Hong H, Wen Y, Lai Y, et al. LL-37 promotes neutrophil extracellular trap formation in chronic rhinosinusitis with nasal polyps. Clin Exp Allergy. 2019;49(7):990-9.
23. Wang X, Sima Y, Zhao Y, Zhang N, Zheng M, Du K, et al. Endotypes of chronic rhinosinusitis based on inflammatory and remodeling factors. J Allergy Clin Immunol. 2022.
24. Lee M, Kim DW, Khalmuratova R, Shin SH, Kim YM, Han DH, et al. The IFN-gamma-p38, ERK kinase axis exacerbates neutrophilic chronic rhinosinusitis by inducing the epithelial-to-mesenchymal transition. Mucosal Immunol. 2019;12(3):601-11.
25. Weckbach LT, Grabmaier U, Uhl A, Gess S, Boehm F, Zehrer A, et al. Midkine drives cardiac inflammation by promoting neutrophil trafficking and NETosis in myocarditis. J Exp Med. 2019;216(2):350-68.
26. Albrengues J, Shields MA, Ng D, Park CG, Ambrico A, Poindexter ME, et al. Neutrophil extracellular traps produced during inflammation awaken dormant cancer cells in mice. Science. 2018;361(6409).
27. Xia X, Zhang Z, Zhu C, Ni B, Wang S, Yang S, et al. Neutrophil extracellular traps promote metastasis in gastric cancer patients with postoperative abdominal infectious complications. Nat Commun. 2022;13(1):1017.
28. Ordovas-Montanes J, Dwyer DF, Nyquist SK, Buchheit KM, Vukovic M, Deb C, et al. Allergic inflammatory memory in human respiratory epithelial progenitor cells. Nature. 2018;560(7720):649-54.
29. Gerdes J, Lemke H, Baisch H, Wacker HH, Schwab U, Stein H. Cell cycle analysis of a cell proliferation-associated human nuclear antigen defined by the monoclonal antibody Ki-67. J Immunol. 1984;133(4):1710-5.
30. Yang A, Kaghad M, Wang Y, Gillett E, Fleming MD, Dotsch V, et al. p63, a p53 homolog at 3q27-29, encodes multiple products with transactivating, death-inducing, and dominant-

Journal Pre-proof

negative activities. Mol Cell. 1998;2(3):305-16.
31. McKeon F. p63 and the epithelial stem cell: more than status quo? Genes Dev. 2004;18(5):465-9.
32. Packard A, Schnittke N, Romano RA, Sinha S, Schwob JE. DeltaNp63 regulates stem cell dynamics in the mammalian olfactory epithelium. J Neurosci. 2011;31(24):8748-59.
33. Kaneko Y, Kohno T, Kakuki T, Takano KI, Ogasawara N, Miyata R, et al. The role of transcriptional factor p63 in regulation of epithelial barrier and ciliogenesis of human nasal epithelial cells. Sci Rep. 2017;7(1):10935.
34. Pokorna Z, Vyslouzil J, Hrabal V, Vojtesek B, Coates PJ. The foggy world(s) of p63 isoform regulation in normal cells and cancer. J Pathol. 2021;254(4):454-73.
35. Su X, Paris M, Gi YJ, Tsai KY, Cho MS, Lin YL, et al. TAp63 prevents premature aging by promoting adult stem cell maintenance. Cell Stem Cell. 2009;5(1):64-75.
36. Wee JH, Ko YK, Khalmuratova R, Shin HW, Kim DW, Rhee CS. Effect of lipopolysaccharide and polyinosinic:polycytidylic acid in a murine model of nasal polyp. Sci Rep. 2021;11(1):1021.
37. Metzler KD, Goosmann C, Lubojemska A, Zychlinsky A, Papayannopoulos V. A myeloperoxidase-containing complex regulates neutrophil elastase release and actin dynamics during NETosis. Cell Rep. 2014;8(3):883-96.
38. Bae JS, Ryu G, Kim JH, Kim EH, Rhee YH, Chung YJ, et al. Effects of Wnt signaling on epithelial to mesenchymal transition in chronic rhinosinusitis with nasal polyp. Thorax. 2020;75(11):982-93.
39. Khalmuratova R, Lee M, Mo JH, Jung Y, Park JW, Shin HW. Wogonin attenuates nasal polyp formation by inducing eosinophil apoptosis through HIF-1alpha and survivin suppression. Sci Rep. 2018;8(1):6201.
40. Hatchwell L, Girkin J, Dun MD, Morten M, Verrills N, Toop HD, et al. Salmeterol attenuates chemotactic responses in rhinovirus-induced exacerbation of allergic airways disease by modulating protein phosphatase 2A. J Allergy Clin Immunol. 2014;133(6):1720-7.
41. Yuan L, Liu H, Du X, Yao Y, Qin L, Xia Z, et al. Airway epithelial ITGB4 deficiency induces airway remodeling in a mouse model. J Allergy Clin Immunol. 2023;151(2):431-46 e16.
42. Aikawa N, Kawasaki Y. Clinical utility of the neutrophil elastase inhibitor sivelestat for the treatment of acute respiratory distress syndrome. Ther Clin Risk Manag. 2014;10:621-9.
43. Chiang CC, Korinek M, Cheng WJ, Hwang TL. Targeting Neutrophils to Treat Acute Respiratory Distress Syndrome in Coronavirus Disease. Front Pharmacol. 2020;11:572009.
44. Wagener JS, Kupfer O. Dornase alfa (Pulmozyme). Curr Opin Pulm Med. 2012;18(6):609-14.
45. Enriquez A, Chu IW, Mellis C, Lin WY. Nebulised deoxyribonuclease for viral bronchiolitis in children younger than 24 months. Cochrane Database Syst Rev. 2012;11(11):CD008395.
46. Lee M, Park CG, Huh BK, Kim SN, Lee SH, Khalmuratova R, et al. Sinonasal Delivery of Resveratrol via Mucoadhesive Nanostructured Microparticles in a Nasal Polyp Mouse Model. Sci Rep. 2017;7:40249.
47. Shin HW, Cho K, Kim DW, Han DH, Khalmuratova R, Kim SW, et al. Hypoxia-inducible factor

Journal Pre-proof

1 mediates nasal polypogenesis by inducing epithelial-to-mesenchymal transition. Am J Respir Crit Care Med. 2012;185(9):944-54.

48. Shin HW, Kim DK, Park MH, Eun KM, Lee M, So D, et al. IL-25 as a novel therapeutic target in nasal polyps of patients with chronic rhinosinusitis. J Allergy Clin Immunol. 2015;135(6):1476-85 e7.
49. Wan T, Zhao Y, Fan F, Hu R, Jin X. Dexamethasone Inhibits S. aureus-Induced Neutrophil Extracellular Pathogen-Killing Mechanism, Possibly through Toll-Like Receptor Regulation. Front Immunol. 2017;8:60.
50. Lapponi MJ, Carestia A, Landoni VI, Rivadeneyra L, Etulain J, Negrotto S, et al. Regulation of neutrophil extracellular trap formation by anti-inflammatory drugs. J Pharmacol Exp Ther. 2013;345(3):430-7.
51. Masso-Silva JA, Sakoulas G, Olay J, Groysberg V, Geriak M, Nizet V, et al. Abrogation of neutrophil inflammatory pathways and potential reduction of neutrophil-related factors in COVID-19 by intravenous immunoglobulin. Front Immunol. 2022;13:993720.
52. Kim SY, Shin DU, Eom JE, Jung SY, Song HJ, Lim KM, et al. Artemisia gmelinii Attenuates Lung Inflammation by Suppressing the NF-kappaB/MAPK Pathway. Antioxidants (Basel). 2022;11(3).
53. Vargas A, Boivin R, Cano P, Murcia Y, Bazin I, Lavoie JP. Neutrophil extracellular traps are downregulated by glucocorticosteroids in lungs in an equine model of asthma. Respir Res. 2017;18(1):207.
54. Gal Z, Gezsi A, Pallinger E, Visnovitz T, Nagy A, Kiss A, et al. Plasma neutrophil extracellular trap level is modified by disease severity and inhaled corticosteroids in chronic inflammatory lung diseases. Sci Rep. 2020;10(1):4320.
55. Zhao L, Li YY, Li CW, Chao SS, Liu J, Nam HN, et al. Increase of poorly proliferated p63(+) /Ki67(+) basal cells forming multiple layers in the aberrant remodeled epithelium in nasal polyps. Allergy. 2017;72(6):975-84.
56. Li CW, Shi L, Zhang KK, Li TY, Lin ZB, Lim MK, et al. Role of p63/p73 in epithelial remodeling and their response to steroid treatment in nasal polyposis. J Allergy Clin Immunol. 2011;127(3):765-72 e1-2.
57. Arason AJ, Jonsdottir HR, Halldorsson S, Benediktsdottir BE, Bergthorsson JT, Ingthorsson S, et al. deltaNp63 has a role in maintaining epithelial integrity in airway epithelium. PLoS One. 2014;9(2):e88683.
58. Fletcher RB, Prasol MS, Estrada J, Baudhuin A, Vranizan K, Choi YG, et al. p63 regulates olfactory stem cell self-renewal and differentiation. Neuron. 2011;72(5):748-59.
59. Sethi I, Romano RA, Gluck C, Smalley K, Vojtesek B, Buck MJ, et al. A global analysis of the complex landscape of isoforms and regulatory networks of p63 in human cells and tissues. BMC Genomics. 2015;16:584.
60. Pecorari R, Bernassola F, Melino G, Candi E. Distinct interactors define the p63 transcriptional signature in epithelial development or cancer. Biochem J. 2022;479(12):1375-92.

Journal Pre-proof

61. Chen Y, Li Y, Peng Y, Zheng X, Fan S, Yi Y, et al. DeltaNp63alpha down-regulates c-Myc modulator MM1 via E3 ligase HERC3 in the regulation of cell senescence. Cell Death Differ. 2018;25(12):2118-29.
62. Fukumoto J, Sidramagowda Patil S, Krishnamurthy S, Saji S, John I, Narala VR, et al. Altered expression of p63 isoforms and expansion of p63- and club cell secretory protein-positive epithelial cells in the lung as novel features of aging. Am J Physiol Cell Physiol. 2019;316(4):C492-C508.
63. Toussaint M, Jackson DJ, Swieboda D, Guedan A, Tsourouktsoglou TD, Ching YM, et al. Host DNA released by NETosis promotes rhinovirus-induced type-2 allergic asthma exacerbation. Nat Med. 2017;23(6):681-91.
64. Radermecker C, Sabatel C, Vanwinge C, Ruscitti C, Marechal P, Perin F, et al. Locally instructed CXCR4(hi) neutrophils trigger environment-driven allergic asthma through the release of neutrophil extracellular traps. Nat Immunol. 2019;20(11):1444-55.
65. Ryu G, Mo JH, Shin HW. Epithelial-to-mesenchymal transition in neutrophilic chronic rhinosinusitis. Curr Opin Allergy Clin Immunol. 2021;21(1):30-7.
66. Martins-Cardoso K, Almeida VH, Bagri KM, Rossi MID, Mermelstein CS, Konig S, et al. Neutrophil Extracellular Traps (NETs) Promote Pro-Metastatic Phenotype in Human Breast Cancer Cells through Epithelial-Mesenchymal Transition. Cancers (Basel). 2020;12(6).
67. Zhu T, Zou X, Yang C, Li L, Wang B, Li R, et al. Neutrophil extracellular traps promote gastric cancer metastasis by inducing epithelial-mesenchymal transition. Int J Mol Med. 2021;48(1).
68. Pandolfi L, Bozzini S, Frangipane V, Percivalle E, De Luigi A, Violatto MB, et al. Neutrophil Extracellular Traps Induce the Epithelial-Mesenchymal Transition: Implications in Post-COVID-19 Fibrosis. Front Immunol. 2021;12:663303.
69. Zuo H, Trombetta-Lima M, Heijink IH, van der Veen C, Hesse L, Faber KN, et al. A-Kinase Anchoring Proteins Diminish TGF-beta(1)/Cigarette Smoke-Induced Epithelial-To-Mesenchymal Transition. Cells. 2020;9(2).
70. Lee M, Lim S, Kim YS, Khalmuratova R, Shin SH, Kim I, et al. DEP-induced ZEB2 promotes nasal polyp formation via epithelial-to-mesenchymal transition. J Allergy Clin Immunol. 2022;149(1):340-57.
71. Zhao R, Fallon TR, Saladi SV, Pardo-Saganta A, Villoria J, Mou H, et al. Yap tunes airway epithelial size and architecture by regulating the identity, maintenance, and self-renewal of stem cells. Dev Cell. 2014;30(2):151-65.
72. Zhou Y, Jiang Y, Peng W, Li M, Chen H, Chen S. The diverse roles of YAP in the regulation of human nasal epithelial remodeling. Tissue Cell. 2021;72:101592.
73. Haas M, Gomez Vazquez JL, Sun DI, Tran HT, Brislinger M, Tasca A, et al. DeltaN-Tp63 Mediates Wnt/beta-Catenin-Induced Inhibition of Differentiation in Basal Stem Cells of Mucociliary Epithelia. Cell Rep. 2019;28(13):3338-52 e6.
74. Pieterse E, Rother N, Garsen M, Hofstra JM, Satchell SC, Hoffmann M, et al. Neutrophil Extracellular Traps Drive Endothelial-to-Mesenchymal Transition. Arterioscler Thromb Vasc

Biol. 2017;37(7):1371-9.

Journal Pre-proof

FIGURE LEGENDS

FIG 1. Presence of NETs in nasal tissues and nasal fluid from patients with CRS. **A**, Immunofluorescence staining of human nasal tissues for NETs. NE (red), CitH3 (green), and DAPI (blue). White arrows indicate NETs. Yellow arrows indicate intact neutrophils. **B**, Quantification of NE+ CitH3+ NET cells. Quantification data of NETs photographed at ×400 magnification. Scale bar = 20 μm. **C**, Protein intensity of NET components in nasal secretions. **B** and **C**, Data are presented as mean ± SEM. Mann-Whitney *U* test. *n.s.*, not significant, **P*<0.05, ***P*<0.01, ****P*<0.001. **D**, Correlation of neutrophil granule protein intensity and extracellular histone intensity. Spearman correlation test.

FIG 2. Location of NETs in human nasal tissues. **A**, Representative immunofluorescence images of NETs in nasal tissue. White bidirectional arrows indicate the distance from NETs in subepithelium to the basement membrane. Yellow bidirectional arrow indicates the distance from NETs in epithelium to the basement membrane. **B**, Measurement of the NETs' location from the basement membrane. Scale bar = 20 μm.

FIG 3. NET levels were correlated with p63+ basal cell expression. **A**, Representative immunofluorescence images of p63 (white), NE (red), and CitH3 (green) in human nasal tissues. Quantification data of NETs, basal cells, and basal cell layers photographed at ×200 magnification. **B**, Correlation of the basal cell layers and the number of NETs. **C**, Correlation of the number of basal cells and the number of NETs. The number of basal cells and NETs were counted per high-power field. Scale bar = 50 μm. Spearman correlation test.

FIG 4. NETs promote an increase of p63+ basal cells. **A**, Scheme of NET treatment in air-liquid interface-cultured hNECs. **B**, Representative immunofluorescence micrographs of p63 (white) and E-

Journal Pre-proof

cadherin (green) expression in hNECs. Scale bars = 50 μm. **C** and **D**, Quantification of p63+ cells and cell thickness (n = 5). **E**, Representative immunofluorescence images of Ki-67 (green) and p63 (red) in hNECs. Scale bars = 50 μm. **F**, Quantification of Ki-67+ p63+ cells (n = 5). **G**, Relative TAp63 and ΔNp63 mRNA expression in hNECs. **H**, Representative immunoblots of ΔNp63 isoforms. **I**, Protein intensity was measured using ImageJ (n = 10). Scale bars = 50 μm. All data are presented as mean ± SEM. Paired Wilcoxon signed-rank test. **P*<0.05, ***P*<0.01.

FIG 5. NETs exist at high levels in a neutrophilic NP murine model. **A**, Schematic diagram of the neutrophilic NP model. **B**, Representative H&E staining images of the nasal cavity. Scale bar = 1000 μm. Areas indicated with squares are shown as magnified images. Scale bar = 200μm. **C**, Numbers of nasal polypoid lesions. **D**, Representative immunofluorescence images of NETs in mouse nasal tissues. MPO (red), CitH3 (green). Scale bar = 50 μm. **E**, Numbers of infiltrated neutrophils. **F**, Numbers of NETs. Data are presented as mean ± SEM. Mann-Whitney *U* test. *n.s*., not significant, **P*<0.05, ***P*<0.01.

FIG 6. NET inhibitors attenuate basal cell hyperplasia in an *in vivo* and *ex vivo*. Immunohistochemical staining images of **A**, p63 and **C**, ΔNp63 in mouse nasal tissues. Representative images photographed at ×1000 magnification. Scale bar = 50 μm. **B** and **D**, Positive cells in the epithelium were counted per HPF (×400 magnification). Data are presented as mean ± SEM. Mann-Whitney *U* test. **E**, Representative immunofluorescence micrographs of p63 (white) and E-cadherin (green) in hNECs. Scale bars = 50 μm. **F** and **G**, Quantification of p63+ cells and cell thickness (n = 6). Data are presented as mean ± SEM. Paired Wilcoxon signed-rank test. *n.s*., not significant, **P*<0.05, ***P*<0.01.

Journal Pre-proof

Lim et al, Fig 1

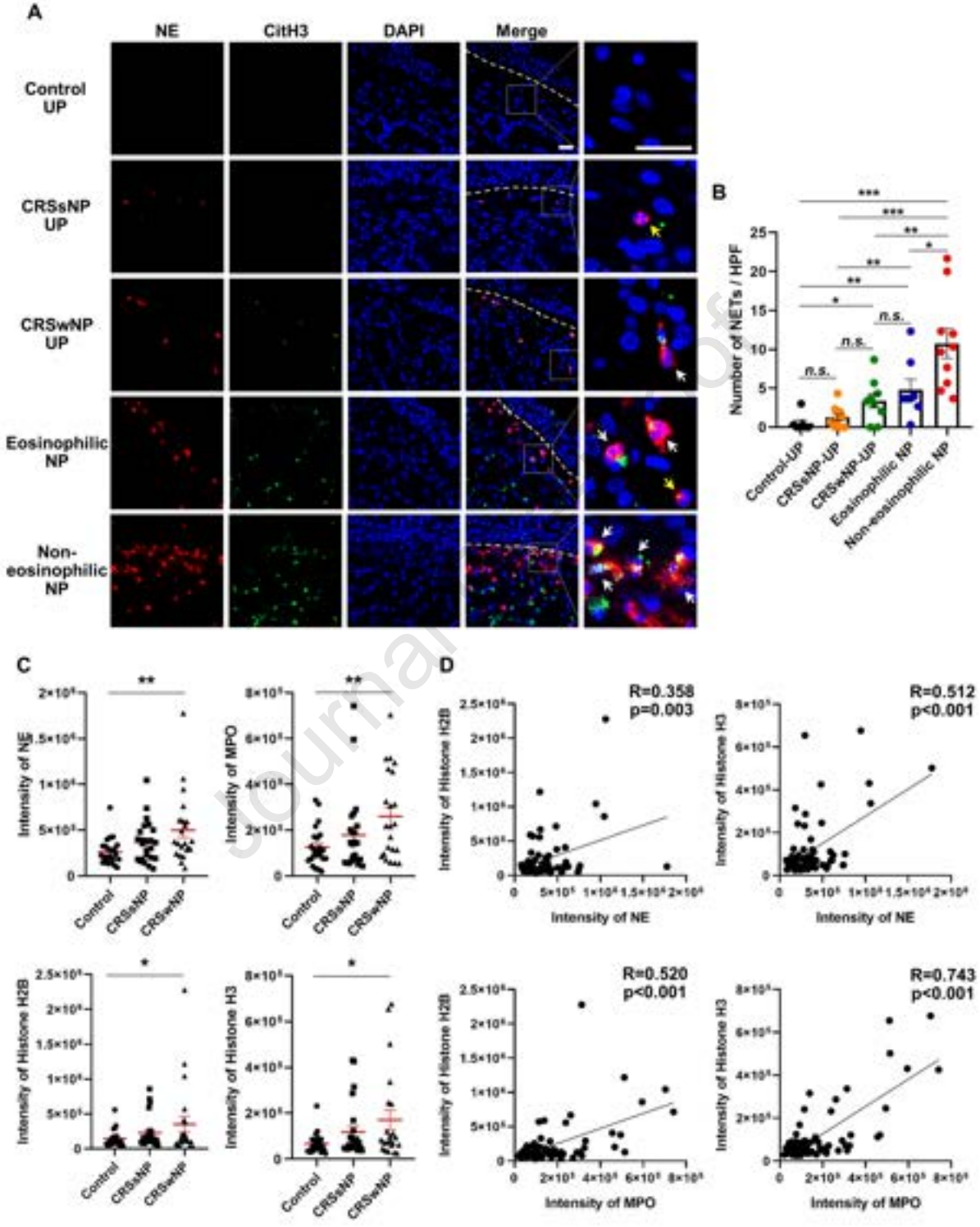

Lim et al, Fig 2

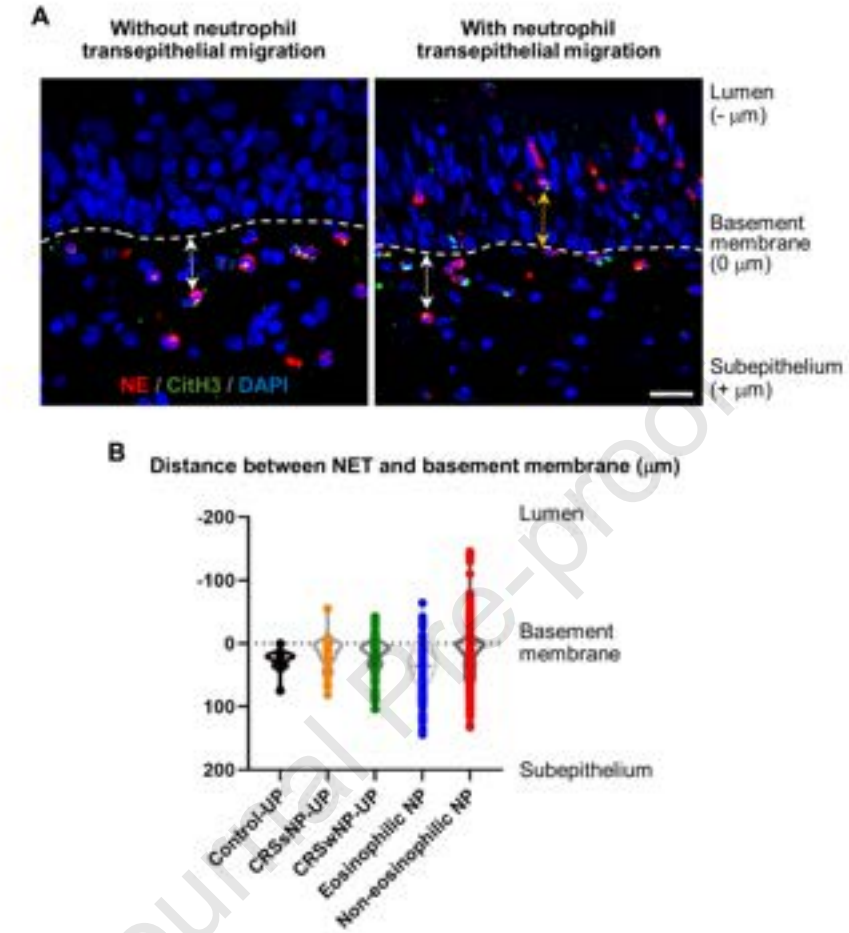

Journal Pre-proof

Lim et al, Fig 3

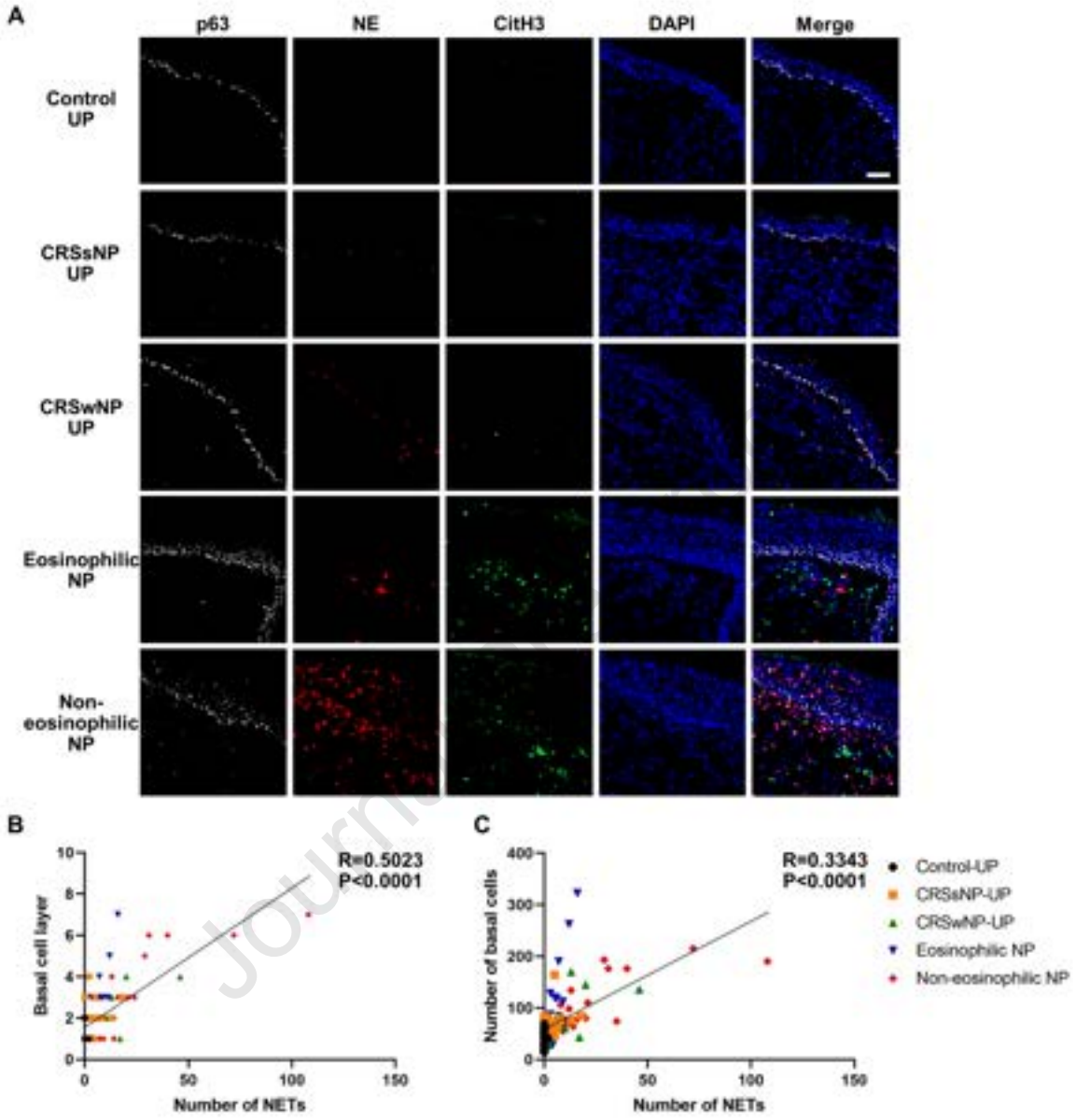

Lim et al, Fig 4

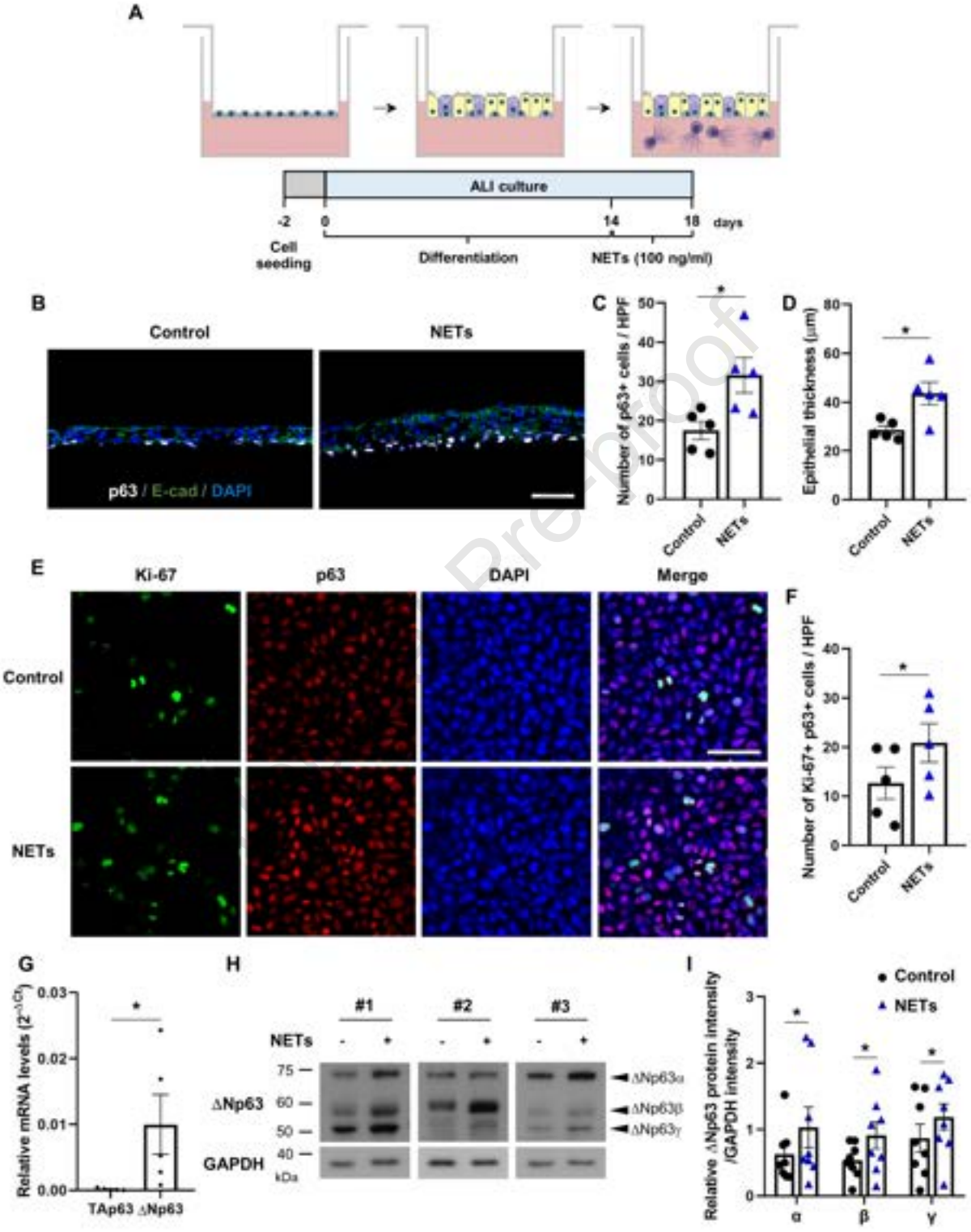

Pre-proof

Lim et al, Fig 5

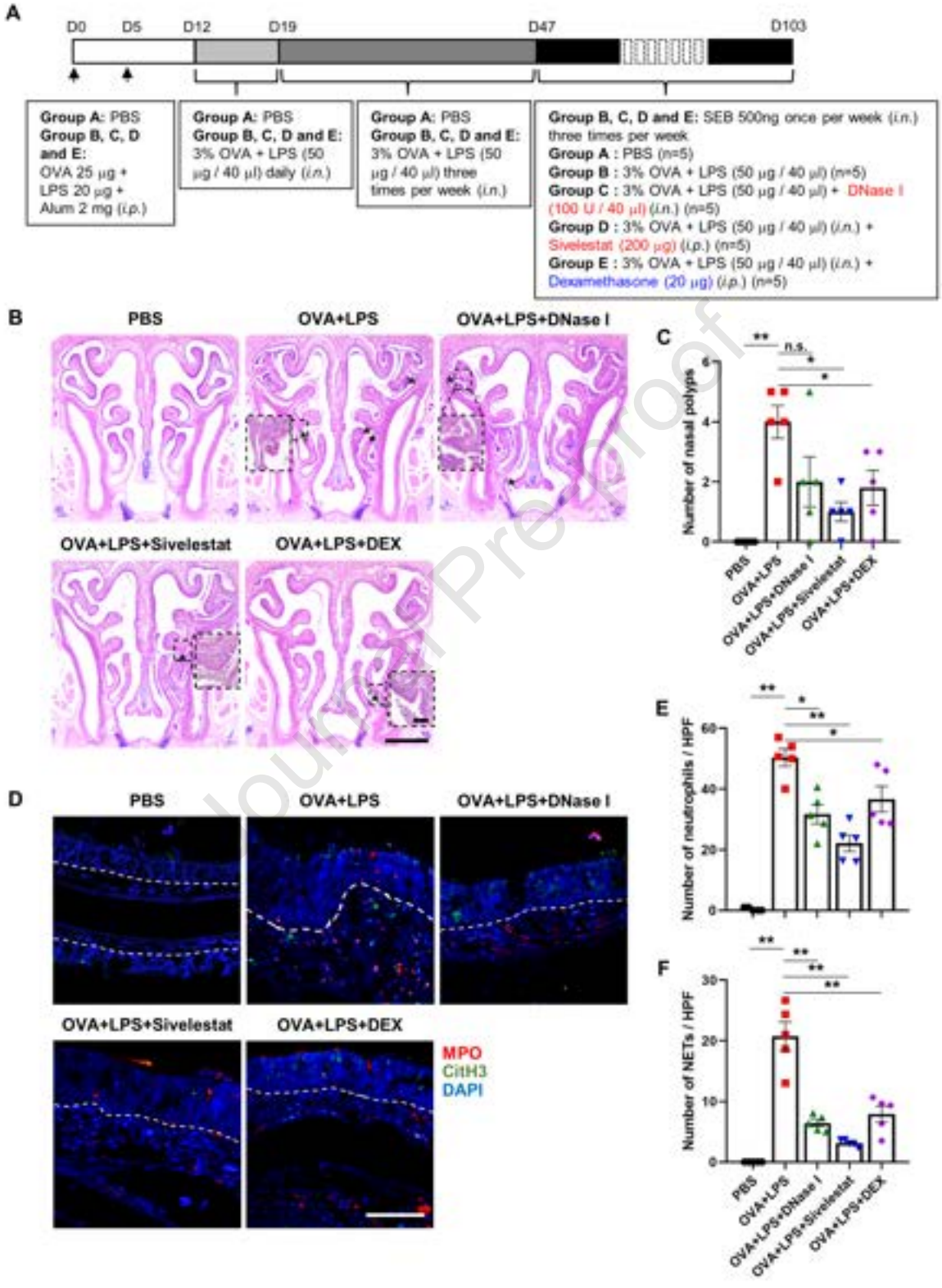

Lim et al, Fig 6

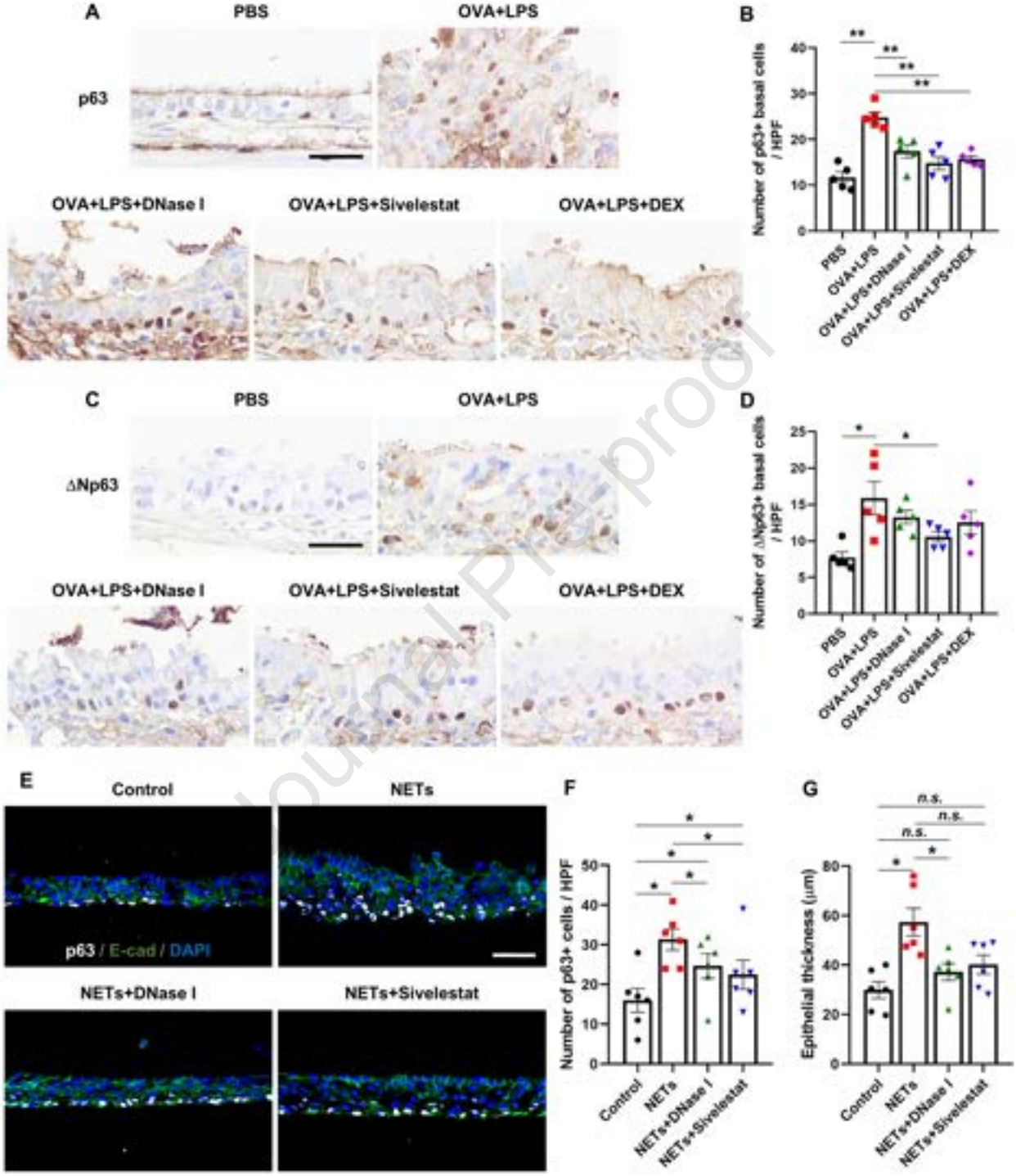

Journal Pre-proof

The Journal of Allergy and Clinical Immunology

Online supplement

Neutrophil extracellular traps promote ΔNp63+ basal cell hyperplasia in chronic rhinosinusitis

Authors: Suha Lim, BSc,[1,2,3] Roza Khalmuratova, MD, PhD,[1] Yun Young Lee, BSc,[6] Yi Sook Kim, BSc,[1,2,3] Mingyu Lee, PhD,[1,2,3,11] Na Kyeong Lee, BSc,[7,8] Se-Na Kim, PhD,[9] Young Bin Choy, PhD,[6] Chun Gwon Park, PhD,[7,8] Dae Woo Kim,[5,10] and Hyun-Woo Shin, MD, PhD[1,2,3,4.5]*

Journal Pre-proof

Online Repository Methods

Immunofluorescence and immunohistochemistry staining

Cells were fixed with 4% paraformaldehyde for 10 minutes and permeabilized with Triton X-100 (PBS + 0.5% Triton X-100) for 30 minutes at 37°C. Tissue sections were deparaffinized and rehydrated, and then heat-induced epitope retrieval was then performed by autoclaving at 121°C for 10 minutes in 100 mM citrate buffer (pH 6.0) (Dako, Santa Clara, CA, USA). Tissues were treated with 3% hydrogen peroxide in methanol for 10 minutes. Then, cells or tissues were blocked with 3% bovine serum albumin in PBS for 1 hour at room temperature (RT). The slides were incubated with primary antibodies, including anti-neutrophil elastase (NE; Novus, Centennial, CO, USA), anti-citrullinated histone H3 (CitH3; Novus, Centennial, CO, USA), eosinophil major basic protein (EMBP; Santa Clara, CA, USA), anti-p63 (R&D, McKinley Place NE, MN, USA), anti-p63 (Abcam, Cambridge, UK), anti-ΔNp63 (Biolegend, San Diego, CA, USA), anti-E-cadherin (E-cad; Cell Signaling, Danvers, MA, USA), anti-Ki67 (Novus, Centennial, CO, USA), and anti-myeloperoxidase (MPO; R&D, Minneapolis, MN, USA) at 4°C overnight. For immunofluorescence, this was followed by incubation with secondary antibodies for 1 hour at RT. Antibodies were diluted in blocking buffer, as delineated in detail in Table E2. After that, slides were stained with 4',6-diamidino-2-phenylindole dihydrochloride (DAPI; Sigma, Saint Louis, MO, USA) for 10 minutes. For mounting on slides, we used mounting medium (Dako, Santa Clara, CA, USA) and covered the slides with a cover glass. Images were analyzed using a confocal microscope (LSM 700, Carl Zeiss Microscopy, Göttingen, Germany).

For immunohistochemistry (IHC), tissue samples were stained with a Polink-2 plus HRP Broad kit with DAB (Origene, Rockville, MD, USA) on day 2. Sections were counterstained with Gill's hematoxylin for 3 minutes and dehydrated using ethanol and xylene and covered with Permount mounting medium (Fisher Scientific, Hampton, NH, USA).

To observe the side aspect of hNECs on transwell, we cut the inserts and conducted cryosectioning. Cells were fixed with 4% paraformaldehyde for 10 minutes at RT. We cut the inserts and the inserts were incubated with 30% sucrose (in PBS) at 4°C overnight. The next day, the inserts were incubated

Journal Pre-proof

with 30% sucrose : OCT (Sakura, Tokyo, Japan) = 1 : 1 solution for 1 hour at RT. Fill the molds with OCT and place the inserts into OCT. Freeze with dry ice and store at -80℃. The OCT blocks cryosectioned into 10μm sections.

LC-MS/MS analysis from nasal secretions

The preparation of nasal secretions and liquid chromatography-mass spectrometry (LC-MS/MS) analysis were performed as described in a previous study.[1] Briefly, 100 μL of nasal secretion was centrifuged at 15,000 rpm for 10 minutes at 4℃. The protein concentration was measured by tryprophan fluorescence and 50 μg of nasal proteins was used per sample. Proteins were digested using the 2-step FASP procedure, and pellets were resuspended in SDT buffer (2% SDS, 10mM TCEP, and 50mM CAA in 0.1M Tris pH 8.0). The buffer was exchanged to UA solution (8M urea in 0.1M Tris pH 8.5) and then to 40mM ammonium bicarbonate (ABC) buffer. We performed first digestion using trypsin/LysC mixture at 37℃ overnight and second digestion using trypsin at 37℃ for 2 hours. The peptides were acidified by 10% trifluoroacetic acid and desalted using C18-StageTips as previously reported.[2] The peptides were dried by vacuum dryer and stored at -80℃. LC-MS/MS was analyzed using a Q-exactive plus (Thermo Fisher Scientific, Waltham, MA, USA) followed by an Ultimate 3000 RSLC system (Dionex, Sunnyvale, CA, USA). We dissolved the dried peptides in solvent A (2% acetonitrile and 0.1% formic acid) and ran with a gradient from 8% to 30% in solvent B (80% acetonitrile and 0.1% formic acid) for 90 minutes. The spray voltage was 2.0 kV in the positive ion mode and heated capillary was 320℃. Centroid data were acquired over an m/z range of 400-1,200. We selected neutrophil-specific proteins and histone proteins, which are the most abundant in this data.

Quantitative reverse transcription polymerase chain reaction

Total RNA was extracted from ALI-cultured hNECs using RNeasy Micro kit (Qiagen, Valencia, CA, USA). cDNA was synthesized by 1 μg of RNA using Tetro cDNA synthesis kit (Bioline, London,

Journal Pre-proof

UK), and qPCR was performed with SYBR Green Polymerase Chain Reaction Master Mix (Enzynomics, Daejeon, Korea) following the manufacturer's instructions. Primer sequences were as follows: 5'-AAGATGGTGCGACAAACAAG-3' and 5'-AGAGAGCATCGAAGGTGGAG-3' for TAp63, 5'-GGAAAACAATGCCCAGACTC-3' and 5'-GTGGAATACGTCCAGGTGGC-3' for ΔNp63, 5'-GGATTTGGTCGTATTGGG-3' and 5'-GGAAGATGGTGATGGGATT-3' for housekeeping gene GAPDH.

Western blotting

Cell lysates were electrophoresed on 10% sodium dodecyl sulfate polyacrylamide gel and transferred to polyvinylidene difluoride membrane (Immobilon-P) (Millipore, Bedford, MA, USA). The membranes were blocked an hour at RT with 5% skim milk in Tris-buffered saline with Tween 20 (0.05%) and incubated with the primary antibodies including anti-ΔNp63 (Biolegend, San Diego, CA, USA) and GAPDH (Santa Cruz Biotechnology, Santa Cruz, CA, USA) at 4℃ overnight. Detailed descriptions are listed in Table E2. The membranes were incubated for 1 hour at RT with horseradish peroxidase-conjugated secondary antibodies in blocking solution. After that, the membranes were visualized by Luminata western HRP chemiluminescence substrate (Millipore, Billerica, MA, USA) or ECL reaction kit (GE Healthcare, San Diego, CA, USA). Densitometric analysis of blots were quantified using ImageJ software (NIH Image processing analysis, http://rsb.info.nih.gov/ij/).

Murine neutrophilic nasal polyp model

All animal experiments were approved by the Institutional Animal Care and Use Committee of Seoul National University (SNU-210705-8-1). Male BALB/c mice, aged 4 weeks, were immunized with an intraperitoneal injection of 25 μg of ovalbumin (OVA; Sigma, Saint Louis, MO, USA) and 20 μg of lipopolysaccharide (LPS; Sigma, Saint Louis, MO, USA) in 2 mg of aluminum hydroxide gel (Thermo Fisher Scientific, Rockford, IL, USA) on days 0 and 5, followed by a daily intranasal

instillation from day 12 to 19 with 3% OVA diluted in 40 μL of PBS (n = 20). Negative control mice were challenged by intraperitoneal injection and intranasal administration of PBS (n = 5). Prolonged continuous inflammation was maintained in the experimental mice by the subsequent nasal exposure to 3% OVA and LPS three times a week for 12 consecutive weeks. In addition to 3% OVA, all groups of mice were challenged on a weekly basis with 500 ng of staphylococcal enterotoxin B (SEB; List Biological Laboratories, Campbell, CA, USA) from day 47 to 102. The mice were subdivided into five groups: PBS (group A, negative control; n = 5); LPS + vehicle (group B, NP control; n = 5); LPS + DNase I (nanoparticles) (group C, NP + NET inhibitor; n = 5); LPS + Sivelestat (group D, NP + NET inhibitor; n = 5); and LPS + dexamethasone (DEX) (group E, NP + steroid, once per week; n = 5) from day 47 to 102. Group A was challenged by intranasal administration of 40 μL of PBS. Groups B-E were challenged intranasally with 50 μL of LPS diluted in 40 μL of PBS. Group C additionally received 100 U of DNase I diluted in 40 μL of PBS. We used DNase I-coated PLGA nanoparticles to improve the stability of DNase I. The method for DNase I-coated PLGA nanoparticles is further described below. Group D was challenged with an intraperitoneal injection of 200 μg of Sivelestat. Group E was treated with intraperitoneal injection of 1 mg/kg DEX. The mice were sacrificed 24 hours after the last intranasal administration. The sinonasal specimens were collected and processed according to previously described methods.[3]

Preparation of DNase I-coated PLGA nanoparticles

DNase I (Roche, Basel, Switzerland)-coated PLGA nanoparticles were prepared as previously described.[4] The primary nanoparticles were prepared with PLGA (Durect Corporation, AL, USA), an FDA-approved polymer, via the conventional single emulsification method. To prepare bare nanoparticles, 200 mg of PLGA was dissolved in 5 mL of dichloromethane (DCM) and then poured into a 10 mL solution of 1% polyvinyl alcohol (Sigma, Saint Louis, MO, USA). The resulting polymer solution was sonicated for 10 minutes at 40% amplitude with 1 second on and 1 second off using a Q700 sonicator (Qsonica LLC, Newtown, CT, USA). The prepared emulsions were poured into 5 mL

Journal Pre-proof

of deionized water and residual DCM was allowed to evaporate overnight at room temperature with magnetic stirring. The PLGA nanoparticles (200 mg) were resuspended in 10 mL of 10 mM, pH 8.5 Tris buffer and coated with a bio-adhesive made of polydopamine (Sigma, Saint Louis, MO, USA) (100 mg of dopamine in 1 mL of water) with vigorous stirring at 4℃ for 3 hours. The bio-adhesive nanoparticles were collected by centrifugation at 17,000 rpm for 20 minutes, resuspended in 5 mL of Tris buffer (10 mM, pH 8.5) containing 50 mg DNase I and 50 mg polyethylene glycol, and stirred at 4 ℃ for 3 hours. The resulting DNase I-coated nanoparticles were then collected and washed with distilled water to prepare DNase I-coated PLGA nanoparticles.

Journal Pre-proof

Supplemental Figure Legends

FIG E1. Presence of EETs in nasal tissues from patients with CRS. **A**, Immunofluorescence images of eosinophil major basic protein (EMBP) (red), CitH3 (green), and DAPI (blue). White arrows indicate EETs. Yellow arrow indicates intact eosinophil. **B**, Quantification of EMBP+ CitH3+ EET cells. Quantification data of EETs photographed at ×400 magnification. Scale bar = 20 μm. Data are presented as mean ± SEM. Mann-Whitney *U* test. *n.s*., not significant, **P*<0.05, ***P*<0.01, ****P*<0.001.

FIG E2. NET proteins in nasal secretions classified by CRS endotype. CRS patients were categorized into EDN high and EDN low to the median EDN value. CRSsNP (EDN high) (n = 12), CRSsNP (EDN low) (n = 12), CRSwNP (EDN high) (n = 11), CRSwNP (EDN low) (n = 11). Protein intensity of NET components in nasal secretions. Data are presented as mean ± SEM. Mann-Whitney *U* test. *n.s*., **P*<0.05, ***P*<0.01.

FIG E3. NET levels were associated with basal cell hyperplasia in non-eosinophilic NP. **A**, Correlation of the basal cell layers and the number of NETs in non-eosinophilic NP tissues. **B**, Correlation of the number of basal cells and the number of NETs in non-eosinophilic NP tissues. Spearman correlation test.

FIG E4. NETs increase p63+ basal cells and epithelial thickness time-dependently. **A**, hNECs treated with NETs for the indicated time. p63 (white) and E-cadherin (green). Scale bars = 50 μm. **B** and **C**, Quantification of p63+ cells and cell thickness (n = 6). Data are presented as mean ± SEM. Paired Wilcoxon signed-rank test. *n.s*., not significant, **P*<0.05.

Journal Pre-proof

147 **FIG E5.** NETs induce abnormal epithelial cell thickness. **A**, Representative Z-stack images with DAPI
148 staining of hNECs. **B**, Measurement of height of the DAPI positive area. Scale bar = 20 μm. **C**, Ki-67
149 (green) positive cells increased by NETs (×100 magnification). Scale bar = 50 μm. **D**, Total cell count
150 using a hemocytometer. **B** and **D**, Data are presented as mean ± SEM. Paired Wilcoxon signed-rank test.
151 **P*<0.05.

152

153 **FIG E6.** Goblet cells and eosinophils in neutrophilic NP mouse model tissues. **A**, Representative PAS
154 staining (goblet cells) images. **B**, Representative Sirius red staining (eosinophils) images. Scale bar =
155 100 μm.

156

157 **FIG E7.** Age information of eight control patients and immunoblots of ΔNp63 isoforms.

158

Journal Pre-proof

REFERENCES

1. Kim YS, Han D, Mo JH, Kim YM, Kim DW, Choi HG, et al. Antibiotic-Dependent Relationships Between the Nasal Microbiome and Secreted Proteome in Nasal Polyps. Allergy Asthma Immunol Res. 2021;13(4):589-608.
2. Han D, Jin J, Woo J, Min H, Kim Y. Proteomic analysis of mouse astrocytes and their secretome by a combination of FASP and StageTip-based, high pH, reversed-phase fractionation. Proteomics. 2014;14(13-14):1604-9.
3. Kim DW, Khalmuratova R, Hur DG, Jeon SY, Kim SW, Shin HW, et al. Staphylococcus aureus enterotoxin B contributes to induction of nasal polypoid lesions in an allergic rhinosinusitis murine model. Am J Rhinol Allergy. 2011;25(6):e255-61.
4. Lee YY, Park HH, Park W, Kim H, Jang JG, Hong KS, et al. Long-acting nanoparticulate DNase-1 for effective suppression of SARS-CoV-2-mediated neutrophil activities and cytokine storm. Biomaterials. 2021;267:120389.

Journal Pre-proof

174 **Table E1. Patient characteristics**

	Control	CRSsNP	CRSwNP		
Total no. of subjects	N = 27	N = 11	N = 9	N = 8	N = 10
Tissue used	UP	UP	UP	Eosinophilic NP	Non-eosinophilic NP
Age (yr)	40.2	44.3	49.6	56.3	50
Asthma, N	0	3/11 (27.2%)	2/7 (28.6%)	0	0
Aspirin intolerance	0	1/11 (9%)	0	0	0
Nasal steroid	12/27 (44.4%)	4/11 (36.3%)	0	1/8 (12.5%)	2/10 (20%)
Oral steroid	1/27 (3.7%)	1/11 (9%)	1/9 (11.1%)	0	2/10 (20%)
Lund-Mackay CT score	1.6	6.8	11.3	10.1	11.6
Blood eosinophil number (/mm^3)	144.9	282.5	383.2	338.5	182.8
Methodologies used					
Tissue IF	N = 7	N = 11	N = 9	N = 8	N = 10
ALI epithelial culture	N = 20	N = 0	N = 0	N = 0	N = 0

CRSsNP chronic rhinosinusitis without nasal polyp, *CRSwNP* chronic rhinosinusitis with nasal polyp, *UP* uncinate process, *NP* nasal polyp, *CT* computed tomography, *IF* immunofluorescence, *ALI* air-liquid interface

175

176

Journal Pre-proof

177 **Table E2. Antibody list**

Antibody	Cat No.	Vender	Application
E-cadherin (24E10)	3195s	Cell signaling	IF, 1:200
p63	AF1916	R&D	IF, 1:100
p63 (EPR5701)	ab214790	abcam	IHC, 1:100
ΔNp63	619002	Biolegend	WB, 1:1000 IHC, 1:100
GAPDH	sc-47724	Santa Cruz	WB, 1:4000
NE (NP57)	NBP2-50529	Novus	IF, 1:200
MPO	AF3667	R&D	IF, 1:400
CitH3	NB100-57135	Novus	IF, 1:200
Ki-67 (8D5)	NBP2-22112	Novus	IF, 1:100
EMBP (F-6)	sc-365701	Santa Cruz	IF, 1:200
Alexa 488-conjugated rabbit IgG	A-21206	Invitrogen	IF, 1:400
Alexa 555-conjucated mouse IgG	A-31570	Invitrogen	IF, 1:400
Alexa 647-conjucated goat IgG	A-32849	Invitrogen	IF, 1:400
Rabbit IgG HRP	G21234	Invitrogen	WB, 1:5000
Mouse IgG HRP	G21040	Invitrogen	WB, 1:5000

178

179

180

Journal Pre-proof

Lim et al, Fig E1

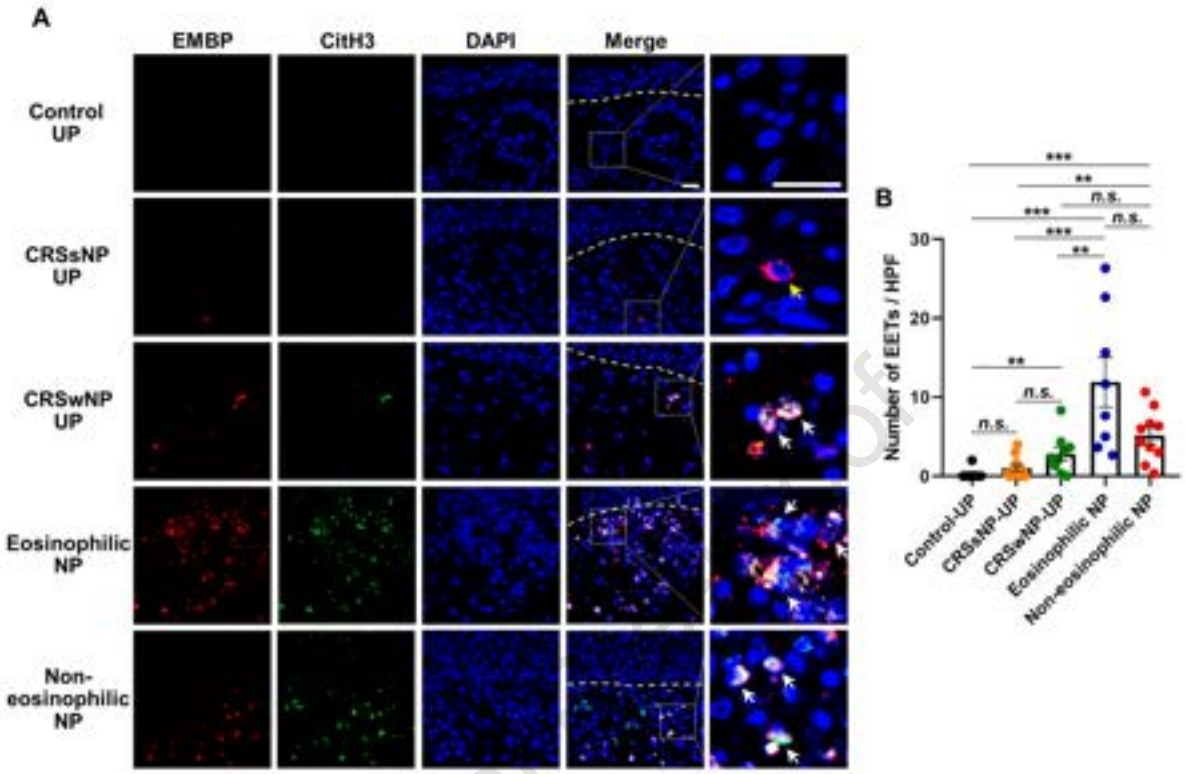

Journal Pre-proof

Lim et al, Fig E2

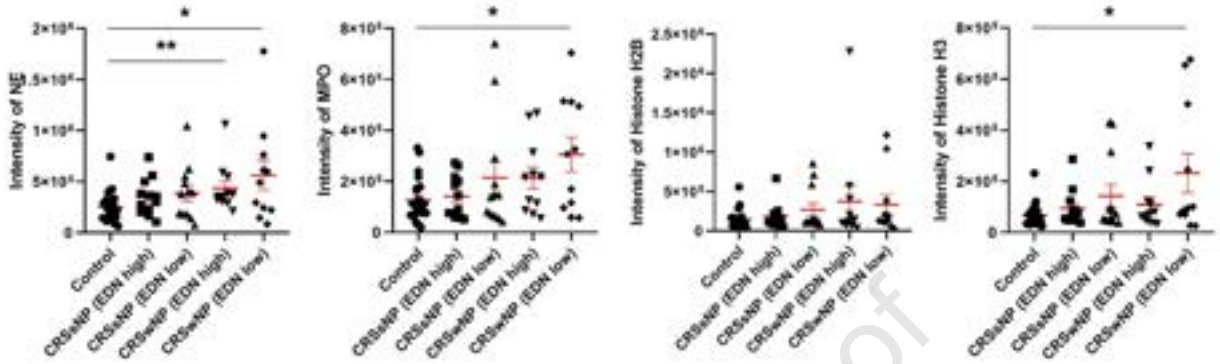

Journal Pre-proof

Lim et al, Fig E3

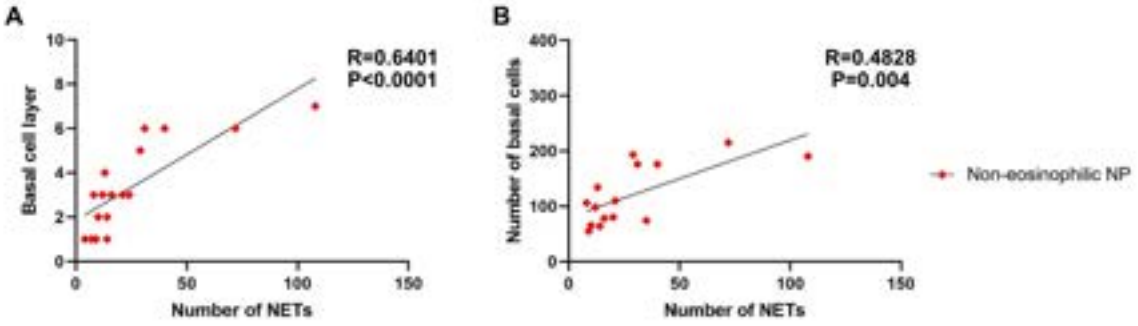

Journal Pre-proof

Lim et al, Fig E4

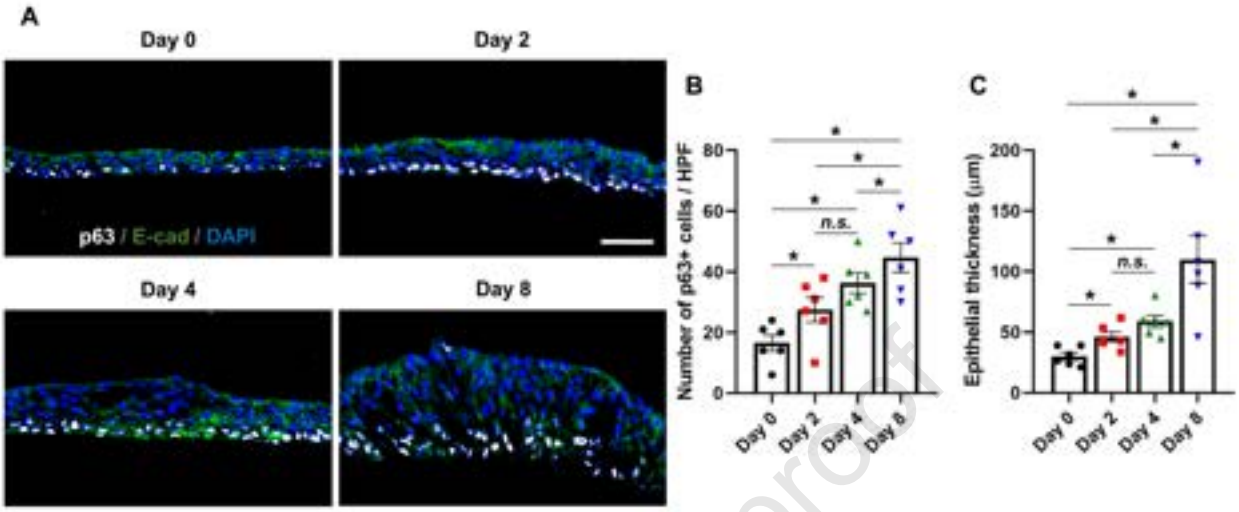

Journal Pre-proof

Lim et al, Fig E5

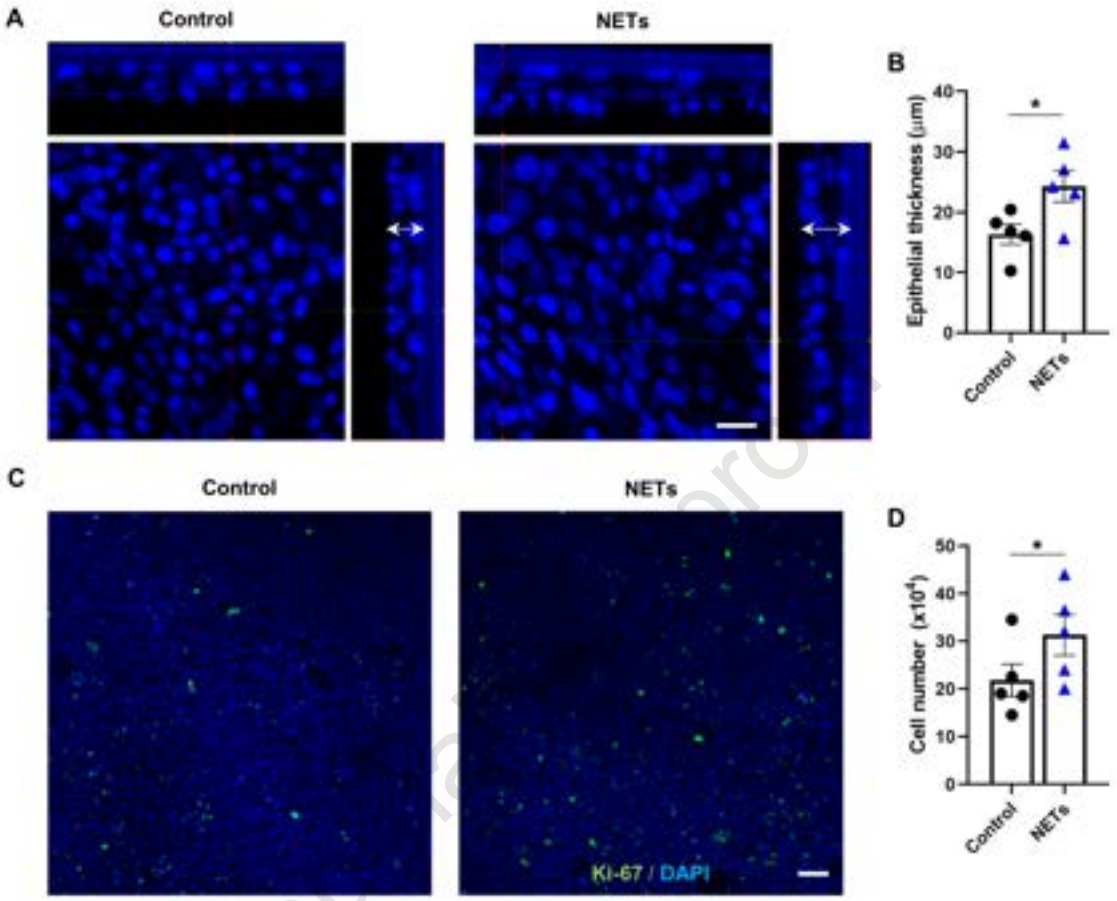

Journal Pre-proof

Lim et al, Fig E6

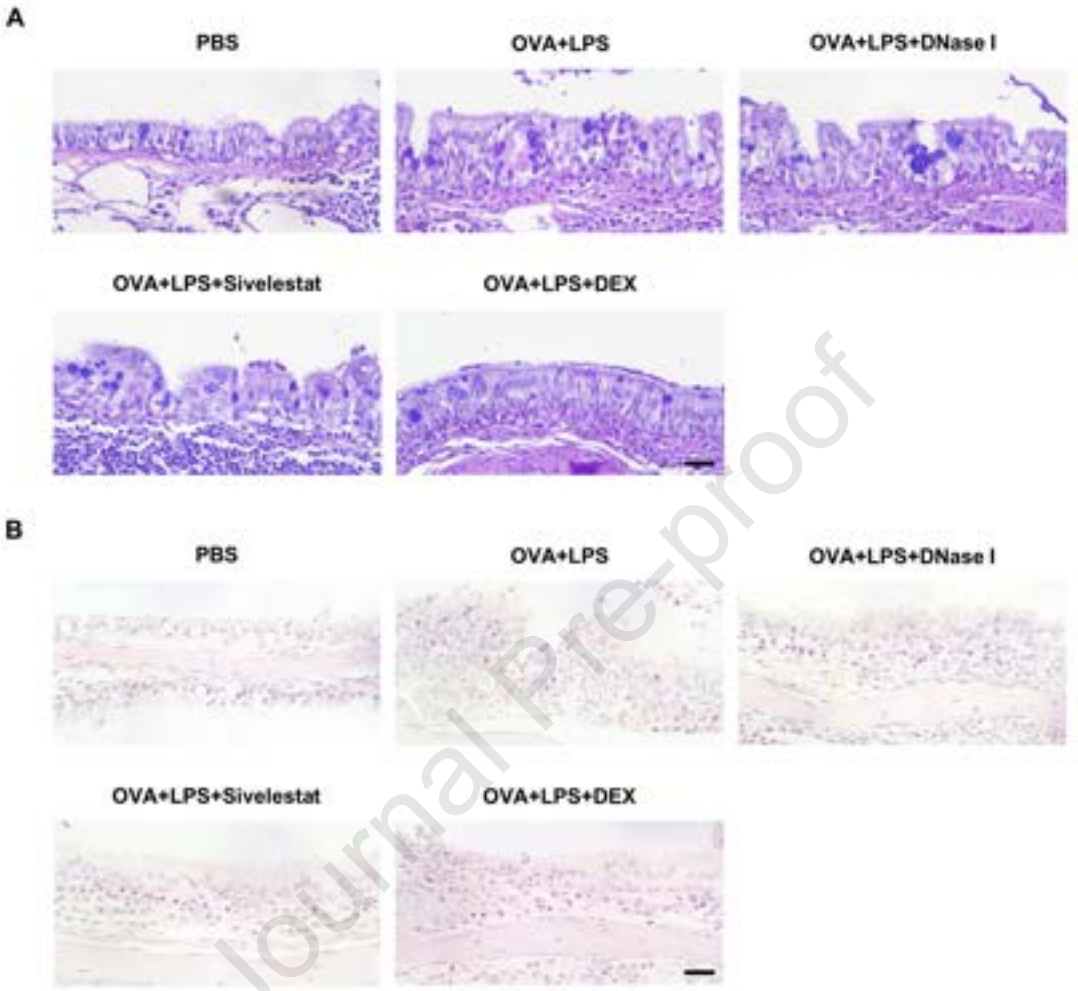

Journal Pre-proof

Lim et al, Fig E7

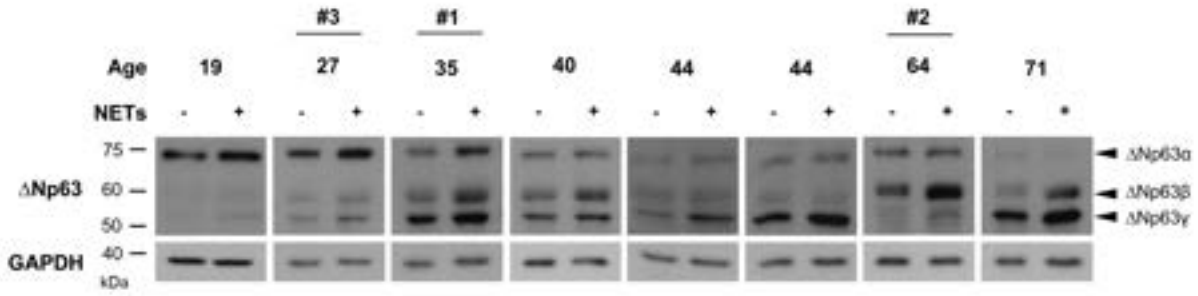

Journal Pre-proof